

Petrographical-geochemical characteristics and floral-faunal compositions of the Valia lignite deposits from Cambay Basin (Gujarat), western India

Vikram P. Singh^a, Bhagwan D. Singh^a, Runcie P. Mathews^a, Vinod A. Mendhe^b, Priya Agnihotri^{a,c}, Subhashree Mishra^d, Malek Radhwani^e, Suryendu Dutta^f, Kumarapuram A. Subramanian^g, Alpana Singh^a, Hukam Singh^{a*}

^aDST-Birbal Sahni Institute of Palaeosciences, 53-University Road, Lucknow-226 007, India

^bCSIR-Central Institute of Mining and Fuel Research, Barwa Road, Dhanbad-826 015, India

^cAcademy of Scientific and Innovative Research, Ghaziabad-201 002, India

^dCSIR-National Institute of Oceanography, Dona Paula, Goa-403 004, India

^eFaculty of Sciences, Department of Geology, Campus Universitaire El-Manar, 2092, Tunis, Tunisia

^fDepartment of Earth Sciences, Indian Institute of Technology Bombay, Powai, Mumbai-400 076, India

^gSouthern Regional Centre, Zoological Survey of India, Chennai-600 028, India

*Corresponding author: *E-mail address*: hukam.singh@bsip.res.in (H. Singh)

Abstract

Lignite-bearing sequence of the Valia mine, associated with the Cambay Shale Formation (early Eocene) in Cambay Basin of western Indian State Gujarat, has been studied. An integrated approach (including organic petrography, palynofacies, palynology, entomology, geochemistry) has been adopted to assess the origin and characters of lignite deposits and their potential for the hydrocarbon generation, besides to understand the evolution and interaction of different biotic (floral-faunal) groups of the geological time. The studied samples (lignites/shales) are characterized by the domination of huminite group (av. 67 vol.%) / phytoclasts (av. 58%) along with the abundance of short-chain *n*-alkanes (bacterial activity). The frequencies of detrohuminite sub-group, non-biostructured elements, macrophyte-derived amorphous organic matter (AOM, mainly), and high values of proxy aqueous are indicating the elevated bacterial degradation of the OM and/or also suggest the significant contribution of the herbaceous vegetation/aquatic macrophytes/algal input to the palaeo-peat. The relative abundance of hopanes and low values of the steroids/hopanoids ratios further indicate a high bacterial activity. On the other hand, the contents of telohuminite, liptinite group, and cuticle elements together with the high carbon preference index, low proxy wax, and terrigenous/aquatic ratios confirm both terrestrial and macrophyte contributions during the peat accumulation. Fascinatingly, we have found *Dipterocarpus*-derived amber (fossil resin) within the lignite seam (lower) with remarkably well-preserved arthropod inclusions consisting of arachnids and insects. Generally, insects have an association with flora and provide important ecosystem functions. In the studied amber samples, the insects to arachnids (spiders and pseudoscorpions) ratio is 3:1. Their quantitative analysis indicates the dominance of the Chironomidae (non-biting midges 32%) followed by Araneae, Myrmicinae, Cecidomyiidae, and Mycetophilidae. A rare entity such as pseudoscorpions has also been found during the investigation.

The derived petrographic indices indicate that the peat-forming limno-telmatic vegetation was accumulated mainly in back-barrier settings with high groundwater (mesotrophic to rheotrophic) condition. The contents of pyrite (mainly framboidal) mineral and sulphur (0.69-2.24 wt.%) suggesting that peat had experienced the marine influx. Further, the high occurrence of funginite maceral (among inertinite group), and spores of family Microthyriaceae point towards a warm and moist condition. The plotting of palynofacies data on Tyson's APP diagram, and the values of pristane/phytane ratio suggest that the OM was primarily deposited in dysoxic to suboxic settings. The high incidence of family Chironomidae, non-biostructured and low cuticle contents indicate the proximal settings and a low energy environment like lake/pond or marshlands. However, the occurrence of granular-AOM along with high (relatively) opaque phytoclast contents in the upper part indicates that distal settings were formed at the termination of the OM accumulation. The total organic carbon (TOC) contents and

hydrogen index values in the studied samples indicate a good to excellent source for the hydrocarbon generation. However, the low gross calorific value (av. 4467 cal/g), values of T_{\max} (mostly below 435 °C), and H/C and O/C atomic ratios showing that the samples are of immature (early diagenetic stage; huminite reflectance value: av. 0.28%) nature of the OM. Moreover, the different cross plots (hydrogen index (HI) vs. oxygen index (OI), S_2 vs. TOC, HI vs. T_{\max}) indicate that the Valia lignite-bearing succession contains admixed type-III/II kerogen, and can generate gaseous and some liquid hydrocarbons upon maturation or with additional heating.

Keywords: Macerals, Palynofacies, Palaeogene-biota, Biomarkers, Proximate-Ultimate analyses, Palaeoenvironment, Depositional setting, Source rock

1. Introduction

The Indian plate detached from Africa (~160 Ma) and Madagascar (~90 Ma) before drifting northward, and collides with Asia resulted in the Tethys ocean's closure and the beginning of the Himalayan orogeny (Rust et al., 2010; and reference therein). Consequently, after breaking away from Africa, the isolated landmass of Indian subcontinent has brought remarkable diversification in the floral and faunal compositions as it has crossed various latitudes and climatic zones (Morley, 2000). Besides, during the early Cenozoic, many catastrophic events occurred, i.e. greenhouse forcing, significant transient warming events, massive change in the global carbon cycle, the enormous release of methane hydrates, etc. (Haq et al., 1987; Kennett and Stott, 1991; Dickens et al., 1995; Svensen et al., 2004; Sluijs et al., 2007; Zachos et al., 2008; Clementz et al., 2011; and references therein). An isolated Indian plate was no exception to these 'terrible' events, and has experienced many of them, e.g. Deccan volcanic (K-Pg boundary), Palaeocene-Eocene Thermal Maximum (PETM) event, etc. These geological events have affected the regional climatic and biotic framework of the subcontinent (Sahni et al., 2006; Rust et al., 2010). Therefore, the deposition of sedimentary sequences of the Palaeogene in western India under the influence of many global events, provided an opportunity to reveal the enthralling history of the geological time.

While straddling the equator (late Palaeocene-early Eocene time; Scotese and Golanka, 1992), the Indian plate was covered with rich and profoundly diverse tropical forests due to the warm and humid equatorial climate (Morley, 2000). Eventually, the thick forest vegetation resulted in lignite deposits (present-day) in western India (in particular), and being mined at several localities, viz. Tadkeshwar (Tarkeshwar), Vastan, Mangrol, Valia and Rajpari (Cambay Basin), Surkha and Khadsaliya (Saurashtra Basin), Matanomadh Panandhro and Umarsar (Kutch (Kachchh) Basin) in the state of Gujarat (Fig. 1a). These deposits not only harbour remarkable palaeo-biota, vital for unraveling mysteries relating to the palaeo-biogeographical history, climatic controls, ecological features, depositional dynamics, but also hold many economically exploitable lignite seams as well as oil/gas fields (Sahni et al., 2006; Rust et al., 2010; Singh et al., 2010, 2017a, b, c; Mathews et al., 2020a; and

many others). Since the discovery of Mumbai High (erstwhile Bombay High) in 1965 by the Oil and Natural Gas Corporation, the Cambay Basin becomes the hotspot for the scientific and industrial communities, and contributes significantly to meet the country's energy demand.

The lignite-bearing sequences of the Cambay Basin have extensively been studied for describing the maceral-mineral matrix and assessing their hydrocarbon potential (Singh et al., 2010, 2012a, b, 2013, 2019; Mallick et al., 2021; many others), biomarker compositions (Dutta et al., 2009, 2011a; Mallick et al., 2021), palynoassemblages (Samant and Phadtare, 1997; Samant and Tapaswi, 2000; Mandal and Guleria, 2006; Garg et al., 2008; Tripathi and Srivastava, 2012; Prasad et al., 2013, 2014; Rao et al., 2013; Shukla et al., 2013; Paul et al., 2015; Singh et al., 2015), fossils wood/fruit (Shukla et al., 2013, 2015; Prasad et al., 2014; Singh et al., 2015; 2016), fossil flowers (Singh et al., 2021) and regional biostratigraphy framework (Sahni et al., 2004, 2006) to understand their nature, origin and depositional environments. Similarly, a large number of significant fauna (vertebrate and invertebrate) have also been recorded from the basin, providing valuable information about the biotic make-up of the geological time, e.g. fishes (Samant and Bajpai, 2001; Bajpai and Kapoor, 2004; Rana et al., 2004; Nolf et al., 2006), ostracods (Bhandari et al., 2005; Nagori et al., 2013), bats (Rana et al., 2005; Smith et al., 2007), Cambaytheres (Bajpai et al., 2006; Rose et al., 2014), lizards (Prasad and Bajpai, 2008), snakes (Rage et al., 2008), rodent (Rana et al., 2008), euprimate (Rose et al., 2009), Avian remains (Mayr et al., 2010), frog (Folie et al., 2013), Acrodontan assemblage (Rana et al., 2013), Tillodont (Rose et al., 2013), etc. Recently, Dutta et al. (2020) have presented evidence of preserved collagen from fish vertebrate in the Cambay Basin.

Studies on the insects (preserved in amber) in accompaniment with the palynoflora have become more decisive in deciphering the evolutionary aspects of related biota (Rust et al., 2010; Smith et al., 2016, Singh, 2020). Alimohammadian et al. (2005) have first examined class II or Dammer-type amber (Dutta et al., 2009; Mallick et al., 2009) of the Cambay Basin. The Cambay amber has records of the earliest social insects and their assemblages (Grimaldi and Singh, 2012, Stebner et al., 2016, 2017; Kania et al., 2017), including the earliest record of Termitidae (Engel et al., 2011) and the oldest fossil record of the sub-family Osoriinae (Coleoptera: Staphylinidae; Ortega-Blanco et al., 2013). Recently, various insect groups in amber have also been examined from the nearby Kachchh Basin with records of true flies (*Chironomus*), social insects, arachnids, and termites (Agnihotri and Singh, 2020; Singh, 2020).

Evidently, notable data have been collected on sediments and amber associated with the Cambay Shale Formation (late Palaeocene-middle Eocene) of Cambay Basin. However, the organic compositions, palaeoecological characteristics, depositional environments, and maturation properties

of the lignite-bearing succession of Valia mine are not sufficiently understood. Nevertheless, Shukla et al. (2015) have recovered the oldest record of *Gynocardia* (fossil wood) from the mine. Hence, to improve the existing knowledge and for further addition to the global database, the present integrated investigation has been conducted. Moreover, this work is the first attempt to study the insect inclusions (in amber) within the studied lignites and associated sediments. This approach will certainly have far-reaching implications to understand the interaction between different biotic groups within the biome and the environments in which they exist. The Valia amber is uniquely diverse, preserving several groups of social insects, spiders, ants, bees, and termites that radiated during the Early Eocene Climatic Optimum and/or during the Palaeocene-Eocene Thermal Maximum (Rust et al. 2010). Although we have found various inclusions, only a few insects have been used for ecological purposes in this study. The detailed taxonomic amber inclusions study will be treated separately.

2. *Geological settings*

The Cambay Basin is one of the most thoroughly studied sedimentary basins of India. The detailed geological framework, age and regional stratigraphy of the basin have already been documented and presented by several workers (Zubov et al., 1966; Krishnan, 1968; Mathur et al., 1968; Chandra and Chowdhary, 1969; Sudhakar and Basu, 1973; Biswas, 1982, 1987, 1999; Raju and Srinivasan, 1983; Roy, 1990; Merh, 1995; Bhandari et al., 2005; Sahni et al., 2006; Punekar and Saraswati, 2010; Rao et al., 2013; and many others). Henceforth, we are briefly describing the geological configuration of the basin.

The Cambay Basin is an intracratonic rift basin with an extent of about 59,000 km² on the west-north-western part of Indian shield in the State of Gujarat, and some part in Rajasthan. The basin is bordered by the Aravalli swell in the northeast, and the Deccan Trap in the east and west (Raju and Srinivasan, 1983). The basin is mainly occupied by Palaeogene sedimentary formations, underlain by the Deccan Traps and overlain by the alluvium. The Deccan Traps are followed by the Vagadkhol/Olpad Formation (Palaeocene–lower Eocene) that contains grey to greyish-green clays and conglomerates, and overlain by the Cambay Shale Formation. Pandey et al. (1993) have classified the Cambay Shale Formation into two units: Older Cambay shale (lower) and Younger Cambay shale (upper; Sahni et al., 2006). The Cambay shale contains many economically exploitable lignite seams along with alternating carbonaceous shale and greyish-green-whitish clay. The age of the Cambay Shale Formation is early Eocene as suggested by Punekar and Saraswati (2010), based on benthic foraminifera (*Nummulites burdigalensis*) from the adjacent Vastan lignite mine. The Cambay shale is overlain by the Amaravati Formation (late Eocene) comprising of nummulitic limestone and marl followed by sub-recent and recent alluviums.

In Valia mine (latitude: 21° 30' 52" N, longitude: 73° 12' 20" E; Fig. 1b), there are two main lignite seams of approximately 3 m (lower seam) and 4.5 m (upper seam) thickness interbedded with carbonaceous and grey shales of variable thickness. A small band of lignite (approx. 0.3 m thick) is also present in between the two main seams. Shukla et al. (2015) have documented the fossil wood from lower seam of the mine. The generalised stratigraphic succession around the study area has been presented in Fig. 2.

3. *Material and methods*

Sums of 51 samples (lignites and associated sediments) were collected vertically in ascending order (channel sampling) from the Valia lignite-bearing succession. The palynofacies and palynology studies were performed on all the samples (Fig. 3). The representative 13 lignite samples, belonging to two seams, were used for the petrographical and bulk-geochemical studies. The Rock-Eval pyrolysis and biomarker (GC-MS) analyses were conducted on 11 and 9 representative samples, respectively.

3.1. *Petrography*

The preparation of particulate pellets of lignite, maceral analyses, and reflectance measurements were carried out following the specifications of ISO standards 7404-2, 7404-3 and 7404-5, respectively (ISO, 2009). The nomenclature of the International Committee for Coal and Organic Petrology (Sýkorová et al., 2005 for huminite group; Pickel et al., 2017 for liptinite group; ICCP, 2001 for inertinite group) has been followed. The rank determination was done following ISO-11760, (2005) standard.

3.2. *Palynofacies*

For the palynofacies study, the samples were treated with HCl (to remove carbonates) and HF (to dissolve silicate) acids, following the method of Batten and Stead (2005). The counted OM (300-500 counts/sample) have been categorized under phytoclast, amorphous OM and palynomorph groups, based on the classification suggested by Tyson (1995), Mendonça Filho et al. (2011), Mendonça and Gonçalves, (2017), using transmitted white light on Leica DM 3000 microscope.

3.3. *Palynology*

The samples were processed for palynological investigation after cleaning from the extraneous matters. The maceration technique of Traverse (1988) was followed for the recovery of palynomorphs. The morphological observation of palynomorphs was performed on prepared permanent slides (mounted with polyvinyl alcohol and Canada balsam) using a Leica DM 3000 microscope. The frequency of each palynotaxa was determined by counting at least 300 palynofossils in every sample.

3.4. Entomology

Amber specimens with arthropod-inclusions were treated via faceting saw (water-fed), grounded on the Buhler's machine with emery sheets multiple grit sizes, following the procedures of Nascimbene and Silverstein (2000). Polishing has been done both manually and with Buhler's machine using viable lubricants. The specimens were observed and photographed under Leica stereomicroscope (LEICA M205A). The specimens rest at the BSIP amber repository.

3.5. Geochemistry

3.5.1. Biomarker analysis

The soluble OM was extracted with dichloromethane: methanol (9:1) mixture from oven-dried powdered lignite/shale samples by ultrasonication for 30 minutes. The precipitation of asphaltenes was performed using an excess of *n*-hexane (40 ml). The separated fractions (saturated and aromatic) have been analysed using an Agilent 7890A gas chromatograph (GC) interfaced to Agilent 5975C mass spectrometer (MS). The procedure described in Singh et al. (2017c) and Mathews et al. (2020a) was followed.

3.5.2. Proximate and GCV analyses

The lignite samples were analysed using micro-balance, oven (for moisture content) and muffle furnace (for ash and volatile matter yields) following the norms of Bureau of Indian Standard IS 1350 (BIS, 2003). The gross calorific values (GCV) were measured on Leco AC 350 GCV analyser according to the ASTM D2015 (1996) norms.

3.5.3. Ultimate analysis

The CHNS values of lignite samples were determined following the D3177-89, D3178-89 and D3179 (ASTM, 1993), respectively on Elementar Vario EL III-CHNS Analyser. The percentage of oxygen was calculated by subtracting the sum of percentages of carbon, hydrogen, nitrogen, ash and sulphur from 100.

3.5.4. Rock-Eval pyrolysis

Pyrolysis experiments were conducted using a "Turbo" Rock-Eval-6 Pyrolyser manufactured by Vinci Technologies®. The procedures of Rock-Eval as suggested by Espitalié et al. (1985) and Lafargue et al. (1998) have been followed.

4. *Results*

4.1. *Petrography*

Values of the observed maceral groups and mineral matter (associated) in the studied lignite samples of Valia mine are presented in Table 1. The illustrations of representative photomicrographs of different maceral types and mineral associations are furnished in Fig. 4.

4.1.1. *Maceral composition*

The maceral analyses showed huminite as the dominant maceral group, ranging between 52 and 75 vol.% (av. 67 vol.%). Among huminite, the detrohuminite (24-49%, av. 37 vol.%) and telohuminite (2-49%, av. 27 vol.%) subgroups have shown dominant occurrences. The gelohuminite subgroup varies from 1 to 8 vol.% (av. 3 vol.%) and is represented only by the corpohuminite maceral. Ulminite is the major maceral (2-47 vol.%) of the telohuminite subgroup. Densinite accounts a significant part (20-48 vol.%) of the detrohuminite content, followed by the maceral attrinite (1-12 vol.%). These lignites also have a considerable proportion of fluorescing huminite or perhydrous huminite (av. 21 vol.%). The liptinite group is moderate (10-24%, av. 18 vol.%) in Valia lignites. Resinite, cutinite, sporinite, suberinite and liptodetrinite are the main macerals of the group, while alginite, bituminite and flourinite (a variety of resinite) macerals are present in traces. The inertinite group is least recorded (1-10%, av. 6 vol.%), and is represented by the macerals funginite, semifusinite and inertodetrinite.

4.1.2. *Mineral matter content*

The mineral inclusions in lignites is relatively low and varies from 4 to 28 vol.% (av. 10 vol.%); mainly represented by the clastics (clay, quartz) and sulphide (pyrite) minerals along with the sporadic presence of carbonate minerals (siderite, calcite). Pyrite (1-8 vol.%) occurs in both framboidal and disseminated forms. The high amount of framboidal types is indicative of the sulphur bacteria activity.

4.1.3. *Rank*

Huminite reflectance is considered as the most accurate rank parameter with the capacity to serve as an independent rank indicator (Suárez-Ruiz et al., 2012). The measured random reflectance (R_r) values of the huminite (ulminite) particles vary from 0.26% to 0.30% (av. 0.28% R_r). The Valia lignites may be categorised as 'low rank-C' as per the ISO-11760-2005 norms.

4.2. *Palynofacies composition*

The components of palynofacies are broadly classified as phytoclasts, amorphous OM (AOM) and palynomorphs for the quantitative analysis. Also, the analysis is carried out according to their size, the degree of degradation/preservation, and optical properties (colouration, opaque, translucent, etc.) in

the lignite and associated sediments. The frequency distribution of particulate OM in the studied samples is listed in Table 2 and presented in Fig. 5. The representative photomicrographs of each OM group are illustrated in Fig. 6.

4.2.1. *Phytoclasts group*

This tissue-derived group is the dominant or subdominant kerogen, ranging between 27 and 87% (av. 61%), in the samples. The non-opaque (translucent) subgroup is more frequent (av. 60%) than the opaque (av. 1%). Among non-opaques phytoclast, non-biostructured is present in good amounts (av. 48%). Its dominance in the non-opaque suggests that the OM may have gone through to pre- and post-depositional alterations (Tyson, 1995). The cuticles are observed in considerable frequency (av. 11%) suggesting a terrestrial influx and proximity to the terrestrial source area (Tyson, 1995). The fungal spores (av. 1%) are also observed in the samples. The opaques (up to 10%) are laths (mainly) types; indicating shorter aerial oxidation (due to the variations in water level and/or selective preservation) during the deposition.

4.2.2. *AOM group*

AOM is the second in abundance of kerogen type, reaching up to 72% (av. 39%) in the samples. This group is mainly represented by the AOM (av. 38%), while the resin subgroup (0-3%) occurs only as an accessory component. The amorphous products subgroup is constituted of those components which do not possess any botanical structures when observed using light microscopy. These components comprise of the degraded products of higher plants tissues (macrophyte-derived AOM), granular-AOM (phytoplankton- and bacterially derived), resinous material of higher plants, microbial mat, and products of extracellular polymeric substances and macrophyte tissues (Tyson, 1995; Mendonça Filho et al., 2011; Mendonça and Gonçalves, 2017).

4.2.3. *Palynomorphs group*

This group represents nil to 4% of the kerogen assemblage in samples, and includes continental (terrestrial and aquatic) components only. The modern affinities assigned to the recorded palynomorphs suggest coastal environmental (brackish water) conditions during the deposition (Singh et al., 2013).

4.2.4. *Palynofacies assemblage*

Based on the quantitative data obtained from the analysed samples, three (I–III) palynofacies zones have been framed in the Valia mine section (Fig. 6; Table 2):

Palynofacies zone-I: The facies occur in sample nos. VA-1-5, 21-34, 36-38, 44 and 47-48, and shows the high frequency of phytoclasts (av. 75%) over AOM elements (av. 24%) of the OM. The palynomorphs are represented in fewer proportions (up to 4%).

Palynofacies zone-II: This facies is recognised in sample nos. VA-6-20, 35, 39-43 and 45. The phytoclasts group (av. 49%) and AOM group (av. 51%) are in co-dominance, while palynomorphs contribute less (up to 1%) to the kerogen composition.

Palynofacies zone-III: The facies is represented by sample nos. VA-49 to 51. It is characterized by high AOM contents (av. 71%) with good preservation. The phytoclasts group is a minor (av. 28%) component in this facies, constituting opaque (av. 8%), woody tissues, cuticles and fungal remains.

4.3. *Palynological assemblage*

The frequencies of major recovered palynotaxa from the Valia mine are presented in Fig.7, and some of them are illustrated in Fig. 8. Although preservation is generally moderate, and richness is relatively low in most of the samples. Over specific intervals of the succession, a notable improvement of productivity is evident. The recorded palynofloras are pteridophytic spores (3 families, 5 species), angiosperm pollen (11 families, 20 species), and fungi (1 family, 2 species), belonging primarily to the tropical-subtropical climatic zone. Amongst them, 6 families are belonging to the thick evergreen rain forest. The angiospermic pollen grains are dominated over the pteridophytic spores in the overall floral composition.

The palynomorph assemblage is represented by angiosperm pollen of the families Arecaceae, Bombaceae, Caesalpinaceae, Miliaceae, Annonaceae and Ctenolophonaceae. The floral assemblage of Arecaceae is mostly abundant in the succession. The pollen grains *Arengapollenites*, *Arecipites*, *Palmidites*, *Longapertites*, *Spinizonocolpites*, etc. of the family Arecaceae indicate dense vegetation within coastal environmental conditions. The recorded pteridophytic spores are of the families Dicksoniaceae, Osmundaceae, Matoniaceae, Polypodiaceae and Schizaeaceae. These families belong to river/stream banks and shady, swampy habitats and water edge habitats. The spores of Schizaeaceae, Matoniaceae along with pollen of Bombaceae, Ctenolophonaceae suggest swampy habitats. The presence of Microthyriaceous fruiting bodies along with fungal remains points to high precipitation in the area.

4.4. *Entomology*

The frequency of recovered arthropods (fossils) is furnished in Table 3, and the representative amber-inclusions from the Valia mine are illustrated in Fig. 9. The ratio of insects to arachnids (spiders) embedded in ambers is 3:1. Various families of insects and spider groups, based on their quantitative

analysis, are as follows: Chironomidae being the dominant group (nematoceran flies, 32%), spiders (25%; families Sicariidae, Actinopodidae), Myrmicinae ants (19%), Cecidomyiidae (biting midges, 13%), Mycetophilidae (fungus gnats, 10%), and the least recorded pseudoscorpions (1%). There are also records of characteristic Eocene freshwater ostracod assemblages from the studied lignite-bearing succession.

4.5. Geochemical parameters

4.5.1. Biomarkers

The biomarkers investigation of the saturated fraction revealed the dominance of *n*-alkanes and hopanes with a consistent presence of triterpenoids. The *n*-alkanes ranges from *n*-C₁₅ to *n*-C₃₁, and observed in the samples with unimodal and bimodal distributions. However, although both distributions are evident, the maximum relative abundance (C_{max}) is shown by *n*-C₁₈ (Fig. 10) except samples V-27 and V-30, where maxima are located in the *n*-C₂₇. Moreover, the *n*-alkanes distribution shows a predominance of short-chain (*n*-C₁₅-C₁₉) over mid-chain (*n*-C₂₁-C₂₅) *n*-alkanes, while long-chain *n*-alkanes (*n*-C₂₇-C₃₁) occur in low quantities.

The various alkane parameters have been calculated and are provided in Table 4. The carbon preference index (CPI: Peters et al., 2005) ranges between 1.60 and 5.94 with an average of 3.12. The terrigenous/aquatic ratio (TAR: Bourbonniere and Meyers, 1996) varies from 0.05 to 1.23 and 2.07 to 2.56 for the shale and carbonaceous shale sediments, respectively. For lignites, the TAR value ranges between 0.07 and 0.26 which is very less considering the nature of the samples. The pristane/phytane (Pr/Ph) ratio varies from 0.43 to 2.01 with an average of 0.99. The proxy wax (P_{wax} : Zheng et al., 2007) varies from 0.22 to 0.70 with an average of 0.50, and the proxy aqueous (P_{aq} : Ficken et al., 2000) varies from 0.47 to 0.88. The aliphatic chain length (ACL) values vary from 15.71 to 23.25 with an average of 20.59.

Terpenoids in the studied samples include bi-, tetra-, pentacyclic triterpenoid and few diterpenoid compounds. The identified bicyclic sesquiterpenoids includes 4 β (H)-eudesmane, 8 β (H)-drimane and C₁₆-compound. The tetracyclic C₂₅- and C₂₆- secohopanes have also been identified. The pentacyclic hopanoid compounds are abundant in the samples. Triterpenoids, other than hopanoids, identified include tetra- and pentacyclic compounds with oleanane, lupane and ursane skeletons. Few aromatic triterpenoids and diterpenoids have also been identified (Table 5).

4.5.2. Proximate, Ultimate and GCV analyses

Table 6 summarizes the data obtained from proximate, gross calorific values (GCVs), and ultimate analyses. The analysis shows that the lignites are high (dry-basis) in moisture contents (15.76-41.70%,

av. 29.06 wt.%), low in ash yields (3.82-19.79%, av. 8.47 wt.%), and moderately high in volatile matter yields (daf: 51.08-75.68 wt.%) and fixed carbon contents (24.32-48.92 wt.%). The fuel ratios (FC/VM) range between 0.32 and 0.96. The GCVs vary from 3279 to 5216 cal/g (av. 4467 cal/g). The studied lignites have relatively high carbon (daf: 58.04-79.07 wt.%) and oxygen (daf: 18.34-34.34 wt.%) contents. The sulphur contents vary from 0.69 to 2.24% (av. 1.52 wt.%; dry-basis). The hydrogen (daf: 2.68-6.56 wt.%) and nitrogen (daf: 0.80-2.90 wt.%) contents have been recorded in lesser amounts. The atomic ratio of hydrogen to carbon (H/C) for the lignites varies from 0.48 and 1.29, whereas the oxygen to carbon (O/C) ratio ranges between 0.19 and 0.44.

4.5.3. Rock-Eval pyrolysis and TOC contents

Pyrolysis experiment has been carried out on the representative samples (7 lignites, 2 carb. shale, 2 shales), covering the entire sequence, and the results are listed in Table 7. The total organic carbon (TOC) contents vary from 35.90 to 55.60 wt.% for lignites, 12.20 to 16.20 wt.% for carbonaceous shales, and from 1.46 to 2.83 wt.% for shales. Information about the OM or kerogen type can reliably be obtained from the hydrogen and oxygen indices (HI and OI). The HI values determined from Rock-Eval pyrolysis vary from 124 to 694 mg HC/gTOC, 278 to 302 mg HC/gTOC, and from 40 to 279 mg HC/gTOC in the lignite, carbonaceous shale, and shale samples, respectively. Whereas, the OI values range between 31 and 69 mg CO₂/gTOC (for lignites), 51 and 58 mg CO₂/gTOC (for carb. shales), and between 59 and 260 mg CO₂/gTOC (for shales). The high HI values of lignites corroborates with their perhydrous nature. This is also reflected in S₂ (remaining hydrocarbon) values of the samples. The lower values of HI in some samples could be due to the type of kerogen present in the sample. The temperature at which the maximum rate of hydrocarbon generation occurs during pyrolysis (T_{max}) indicates the level of thermal maturity, with T_{max} values varying from 379 to 417 °C, 424 to 427 °C and from 433 to 437 °C for the lignite, carbonaceous shale and shale samples, respectively.

5. Discussion

5.1. Palaeovegetation reconstruction

The Valia lignites are composed mainly of the huminite, followed by the liptinite and inertinite groups of macerals suggesting a continuous terrestrial (tress, herbs, shrubs and bushes) influx, deposited/preserved under a relatively high level of ground water at the deposition site. The distribution of *n*-alkanes in organic-rich sediments provides general indications of the OM source, depositional setting and climatic condition (Peters et al., 2005; Mathews et al., 2020b; and many more). Both unimodal and bimodal distributions have been identified in the studied samples along with the presence of short to long-chain *n*-alkanes. This suggests input of OM from the various sources. The high occurrence of the short and intermediate *n*-alkanes chain indicates the important contribution of

algal or bacterial OM and aquatic macrophytes, respectively (Gelpi et al., 1970; Tissot and Welte, 1984, Ficken et al., 2000; Nott et al., 2000). The high values of P_{aq} confirm the important contribution of submerged/floating macrophytes under a considerable water column (Ficken et al., 2000).

Evidences from the palaeobotanical record suggest that the herbs, shrubs and bushes including pteridophytes were grown widely during the Eocene period in western India, as understory floras in the angiosperms-dominant forest (Venkatachala et al., 1969; Mandal and Guleria, 2006; Rao et al., 2013; and others). Further, the dominance of detrohuminite in the studied lignites, reflected by the relatively higher contents of densinite maceral, points towards the significant contribution of herbaceous/bushy plants (decompose easily) in the peat-forming vegetation, deposited in subaqueous conditions. High frequency of biodegraded phytoclasts, an appreciable amount of gelified-AOM, and the presence of pteridophytic palynomorphs belonging to the families Dicksoniaceae, Osmundaceae, Polypodiaceae, Lycopodiaceae, Matoniaceae indicate the predominance of herbs/shrubs source vegetation in the vicinity and/or extremely high-level of bacterial activities. In the palynoassemblages, also the pteridophytic spores reflect the morphological similarities with Cytheaceae, Osmundaceae, Lycopodiaceae families that are limited to tropical-sub-tropical areas (Table 8). However, some of these are cosmopolitan in distribution (Ramanujam, 1995; Rao, 1995). The pteridophytic spores *Osmundacidites*, *Todisporites*, *Polypodiaceasporites*, *Polypodiisporites* jointly specify the presence of humid and shaded habitats with perpetual water in the area (Ramanujam, 1995).

The relatively higher content of maceral funginite along with occurrence of family Microthyriaceae are suggestive of a warm and moist condition, prevailed during the time of peat accumulation. Further, the appreciable contents of perhydrous or fluorescing huminite (decomposed products of liptinite) also indicate the contribution of herbaceous vegetation in the peat formation. On the other hand, the occurrences of ulminite along with the resinite, sporinite and cutinite macerals indicate the existence of higher plants in the surrounding area, and contribute meaningfully to the peat formation. The high CPI values confirm the contribution of continental plants (waxy plants) to the OM (Bray and Evans, 1961; Eglinton and Hamilton, 1967; Caldicott and Eglinton, 1973). Moreover, the average P_{wax} values evidence the noticeable contribution of land plants and macrophytes to the OM.

Similarly, the terpenoid composition in OM is a good indicator of the source floras. The study reveals the large abundance of pentacyclic non-hopanoid triterpenoids and tetracyclic de-A-triterpenoids. These compounds include angiosperm-derived triterpanes, their degradation products. The pentacyclic hopanoid compounds are abundant in the samples, and are dominated by $17\beta(H)$ -22,29,30-Trisnorhopane, 30-Norneohop-13(18)-ene and α , β -Homohopane (Fig. 11). The consistent presence of non-hopanoid triterpenoids of oleanane skeleton suggests the contribution of angiosperms

to the peat biomass (Karrer et al., 1977). Hopanoid distributions indicate the bacterial origin of sedimentary OM (Peters et al., 2005). The biological precursor compounds of hopane derivatives are considered to be bacteriohopantetrol, and to a smaller extent 3-desoxyhopanes (Ourisson et al., 1979; Rohmer et al., 1992). Aerobic bacteria, fungi as well as cryptogams are found to contain these compounds (Bechtel et al., 2001). Secohopanes in the samples are also indicating microbial degradation of the OM.

The TAR values are higher in carbonaceous shales suggesting higher input of terrestrial OM. However, in lignites, low TAR and P_{wax} values point to the less contribution from the higher plants, which is unusual considering the nature of the samples. This discrepancy indicates alteration of the OM characteristics leading to unusual results. On the contrary, more abundance in the long-chain *n*-alkanes is observed in carbonaceous shales than the lignites. This unusually low abundance of long-chain *n*-alkanes in lignite samples could be a probable result of the microbial degradation. Intense bacterial activity leads to the increase of *n*-alkanes shorter than *n*-C₂₃ from higher plants (Otto et al., 1994; Dehmer, 1995). Thus, $\Sigma C_{22-} / \Sigma C_{23+}$ ratio can be an effective indicator of the intensity of microbial degradation. In all the lignite samples, the ratio is greater than 6 and even up to 9.93 (Table 4) suggesting intense bacterial degradation of terrestrial biomass. It has also been observed that the higher microbial degradation favoured the removal of long-chain *n*-alkanes during early diagenesis ~60-80 °C (Zhang, 1979; Peters and Moldowan, 1993), which is indicated by the high relative abundance of short-chain homologues, consequently, leading to the low TAR and P_{wax} (in lignites). On the other hand, the association of pyrite (including framboidal) in the lignites suggests a marine incursion during the peat deposition. The oxygenated water further enhances the bacterial activity in the mire and causes tissue destruction. The high mineral matter contents in top most samples (V-12 and 13) suggest that the high inorganic material is transporting into the mire at the termination point of peat accumulation.

Amber, hugely diverse in its chemical composition of terpenoids (Simoneit et al., 1986, 2016; Mallick et al. 2014) as an outcome of environmental stresses and volcanic activity to be considered as major causes (Naglik et al., 2018 and references therein). The recorded arthropod composition of the Valia amber indicates the prevalence of a tropical forest with the dominance of Dipterothripidae with warmer conditions and high humidity (Dutta et al., 2009; Rust et al., 2010). It also supports the existence of aquatic habitats near the shoreline for the growth of Dipteran flies (Stebner et al., 2017; and references therein). The rare occurrences of crustacean fossil (freshwater ostracods) assemblages includes specimens assigned to family Candonidae and Limnocytheridae. Dating back to the Ordovician (Horne, 2005), these are mostly represented by their calcified bivalved carapace and a

hinge. The soft parts are rare to be recorded due to lack of preservation (Wang et al., 2020). Comparing faunal assemblages depicts true flies as the major element of the Eocene in Cambay Basin. As a result of ectothermy, arachnids and insects can resist variations in the ecosystem. Fossil pseudoscorpions are a rare entity preserved in amber, irrespective of their modern diversity. Trapped in a tree resin, one expects to predominantly get arboreal taxa, bark-associated families, or under rocks (Harms and Dunlop, 2017), responsible for decomposing. They favour development in a warmer climate, similar to those found in warm-temperate or sub-tropical type of conditions. Common to the Cenozoic and early Cretaceous insect assemblage (Sinitshenkova, 2002), records of nematoceran flies in amber value to non-biting midges as ecological and paleoclimate indicators during the Eocene. They largely thrive well in warm-temperate and moist-tropical regions with the dominance of conifers and pines. Here in the studied samples, the presences of *ent*-Kaurane, Isopimarane and 19-norisopimarane compounds (although less) hint the minor contribution of the conifer vegetation. This agrees with the earlier report of Mandal and Guleria, (2006).

The earlier works on Palaeogene/Neogene amber in Southeast Asia is suggestive of dammerane-type resin, exuded from trees of family Dipterocarpaceae (Simoneit et al., 2020 and references therein). According to Kocsis et al. (2020), the FTIR spectra from Indian Eocene dipterocarp Cambay amber (Dutta et al., 2009, 2011b; Rust et al., 2010) is analogous with the Borneo records. Notably, during late Cretaceous the Dipterocarpaceae family was growing abundantly in India and later migrated to Asia (Morley, 2000). Besides, Singh et al. (2017c), have reported the occurrences of tetracyclic diterpenoids with kaurane skeleton in the Eocene Surkha lignite of Saurashtra Basin (Gujarat). These types of compounds predominantly occur in the leaf resins of coniferous tree: *Agathis* (family Araucariaceae; Noble et al., 1985), also reported from Borneo (Kocsis et al., 2020; Simoneit et al., 2020). Therefore, with the similar present-day tropical vegetation, biomarker signature and the geographical emplacement (Latitude: 3° 21' 16" N, Longitude: 117° 35' 47" E; Fig. 12), the peatland/rainforest of Borneo could be considered as a modern equivalent for the Indian Eocene lignite deposits.

5.2. Palaeodepositional condition

Coal/lignite macerals, derived from plant tissues through a gradual process of decomposition and preservation, serve as one of the best tools to understand the botanical framework of the hinterland. They are also useful in deciphering the depositional conditions, and the changes under which the OM has gone through after its burial, such as water table, pH, bacterial activity, degree of the thermal maturation, etc. (Silva et al., 2008; Suárez-Ruizet al., 2012; and references therein). The various maceral-derived indices have effectively been used in reconstructing the depositional conditions

(Kalkreuth et al., 1991; Životić et al., 2010; Suárez-Ruiz, et al., 2012; Singh et al., 2012a, b, 2013, 2017a, b, c; Radhwani et al., 2018; Mathews et al., 2020a; and many others). Although, it is recommended that these indices/facies models be used with caution, and in conjunction with other parameters such as geochemistry, palynofacies, palynology, etc. (Crosdale, 1993; Wüst et al., 2001; Scott, 2002; Moore and Shearer, 2003).

Kalkreuth et al. (1991) and later Kalaitzidis et al. (2004) have modified the gelification index (GI) and tissue preservation index (TPI) facies model for the Palaeogene-Neogene coal, originally proposed by Diessel (1986) to understand the depositional settings of Australian Permian coals. Here, we have used the relation given by Kalaitzidis et al. (2004; refer Table 1). The Valia lignites have high GI values range from 2.52 to 26.47 (av. 7.07) and low TPI values vary between 0.06 and 1.95 (av. 0.85). The plot of these values on Diessel's model suggests that the poorly preserved limnic to limno-telmatic peat vegetation was deposited (mainly) under the back-barrier environment (Fig. 13). A low TPI values suggests either predominance of the herbaceous plants (soft-wood or cellulose-rich) in the mire or large-scale destruction of plant tissues due to the intense humification (Diessel, 1992).

Elevated water-oxygen content leads to increased tissue destruction due to the more intense humification, and results in the preferential formation of detrohuminite over telohuminite in both woody and herbaceous precursor materials (Dehmer, 1995). The domination of non-biostructured components of OM in the studied samples further reinforces the above observation. TPI also indicates pH conditions of palaeomires because, in a low pH condition, microbial activity is weak and plants can be well-preserved, and vice-versa (Zhang et al., 2010). Further, the lower values (<1) may also be attributed to the presence of herbaceous vegetation, also supported by the dominance of detrohuminite (detritus) in the maceral composition.

Furthermore, a moderate variation in the GI values is suggestive of some fluctuation in redox conditions in the basin, probably due to the fluctuations in water cover. It has also been observed that marine-influenced-peat often has a higher content of sulphur (Diessel, 1992). To a greater extent, depositional conditions favour the intensification of microbial activity. Studies have shown that an increase in salinity can be a causative factor (Qin et al., 2010). Thus, it may be assumed that the setting in which the peat mire deposited was under the influence of marine conditions causing the increase in salinity of the mire water leading to sulphate reduction by bacteria. In the investigated samples, the contents of sulphur and pyrite together with ash yields suggesting that peat has experienced the influx of sulphate and Fe-rich sea water in a back-barrier/coastal systems (Kalkreuth et al., 2010).

The groundwater or relative rainfall (hydrological condition) and vegetation type (e.g., trees, bushes) play an important role in the development of peat, and to understand this Calder et al. (1991)

have proposed a facies model based on groundwater (GWI) and vegetation inputs (VI). Here, the GWI and VI equations as specified in Kalaitzidis et al. (2004) has been used, with a slight modification as suggested by Stock et al. (2016) in the GWI equation (see Table 1). The GWI values of lignites range from 0.47 to 2.03 (except for one higher value 18.13, could be due to mineral matter influx and/or intermittent marine influence), and the VI values range from 0.39 to 1.99 suggesting a good, but fluctuating (mesotrophic to rheotrophic), hydrological condition (ground-water level) was prevailing during the deposition of peat (Fig. 14). The low VI values together with relatively less contribution of biostructured phytoclasts and cuticle components in the palynofacies composition reflecting the dominance of herbaceous/soft-wood vegetation that deposited under subaquatic condition. The VI values are more or less uniform throughout the seam sections; suggesting that no significant change in the vegetal input occurs during the peat development.

The relatively low frequencies of recorded inertinite macerals and opaque phytoclasts indicate that the peat surface has experienced an occasional/short period of aerial exposure, which further minimizing the possibility of oxidative degradation of the OM/peat. The Pr vs. Ph ratio provides evidence about the redox conditions of the depositional environment (Didyk et al., 1978). The analysed samples show Pr/Ph ratios <1 , except samples V-27, 30 and V-41. The values indicate the predominance of a dysoxic environment and anaerobic conditions within the deposit environment. The Pr/*n*-C₁₇ vs. Ph/*n*-C₁₈ plot further suggests that the deposits were formed in near-shore conditions (Fig. 15). While, it is supposed that the influence of marine water was not prominent during the deposition of carbonaceous shale. The occurrence of Arecaceae pollen also indicates the near-shore depositional (marginal marine) settings.

Further, the origin of Cambay amber is supposed to have occurred in relatively more humid and warmer climatic conditions (Stebner et al., 2017). Subsequently, the tropical families like Arecaceae, Annonaceae, Bombacaceae, Liliaceae and Ctenolophonaceae are indicative of the warm and humid climate. The palms are arborescent monocotyledons, and considered to be of pantropical origin. Presently, they are predominantly found in tropical-subtropical evergreen and semi-evergreen forest ecosystems (Table 8) across the world (Greenwood and Wings 1995; Morley 2000, 2003; Dransfield et al. 2008). Besides, the appreciable contents of maceral funginite in lignites as well as the occurrence of epiphyllous fungi (Microthyriaceae) mainly indicate moist condition. The records of fossil epiphyllous fungi, such as *Phragmothyrites* and *Callimothallus*, are also indicators of heavy rain (Dilcher 1965; Saxena and Tripathi 2011). These fossil fungi are growing abundantly in tropical-subtropical mesophytic vegetation that thrives in a humid climate with heavy rainfall (Selkirk, 1975). The presence of maceral alginite, derived from algae like *Botryococcus* (fig. 4h), along with the

pteridophytic spores, such as *Dictyophyllidites laevigatus*, *Todiosporites plicatus*, *Dandotiaspora dilate*, etc. are indicative of freshwater swamp and pond conditions.

The record of *Chironomidae* genera and ostracod families in the Valia amber also suggests the presence of freshwater environment and standing water bodies (Stebner et al., 2017; Wang et al., 2020). Earlier records of vertebrate fauna (Rana et al., 2004, 2005; Rose et al., 2006; Sahni et al., 2006) and palynological assemblages (Rao et al., 2013) from the adjacent Vastan mine have also indicated the influx of freshwater during the peat deposition in Cambay Basin. Moreover, the climate is one of the main contributory factors controlling the floral characteristics and hydrological conditions in any environment. It also controls the deposition, formation of OM, and their diagenetic alterations. Thus, in the formation of thick seams of lignite and carbonaceous shales, climate plays a pivotal role. The alkane parameter, ACL (Eglinton and Hamilton, 1967) has been utilized by various workers to elucidate the paleoclimatic conditions. The ACL values strongly reflect the moisture conditions, and may be utilized to know the climatic conditions during the existence of the plant (Anderson et al., 2011; Baker et al., 2016). Hotter and drier conditions contribute to longer ACL values and vice versa (Zhou et al., 2005). The relatively low ACL values (15.71-23.25) in the studied samples suggest wetter conditions, pointing to the humid climatic conditions that existed in the basin which is further supported by the floral and faunal compositions.

Furthermore, the extrapolation of palynofacies data on Tyson's APP (AOM–Phytoclasts–Palynomorphs) diagram revealed the dispersal of samples mainly in three fields (II, VI and IX; Fig. 16), corresponding to the three palynofacies zones (see section 4.2.4) of the studied succession:

Marginal dysoxic-anoxic basin, II (Palynofacies zone-I; lithology: lignite, carb. shale and shale)—characterized by the high frequency of non-biostructures and subordinate amount of cuticles along with the minimum representation of palynomorphs. The AOM (mainly gelified) also contributes significantly to the kerogen composition. The dominance of non-opaque phytoclasts indicates that the deposition of the OM took place in the proximal (to source) settings (Tyson, 1995). The non-biostructured elements are with no botanical structure, translucent, and formed in low-energy conditions like stagnant water/lake/pond (Tyson, 1993; Mendonça and Gonçalves, 2017). Subsequently, the macrophyte-derived AOM are linked to the high bacterial activity that requires an oxygenated environment, but their preservation needs a dysoxic-anoxic basin which could be related to transportation to an oxygen-depleted and stagnant environment. Similarly, the occurrences of major fossil spiders are from the lacustrine or similar quiet-water deposits, where there are least chances of mechanical destruction of soft bodies in the area (Selden and Penney, 2009). Based on these, a low or quiet energy environment (lake/pond, etc.) under proximal settings can be assigned to this facies.

Proximal suboxic-anoxic shelf, VI (Palynofacies zone-II; lithology: lignite and shale)—categorized by the co-dominance of phytoclast and AOM components. The increase in AOM, and decrease in non-biostructured and cuticle contents (w.r.t. Palynofacies-I) indicate an elevated level of OM degradation and/or amorphization in the proximal environment. According to Pacton et al. (2011), prolong darkening conditions (anoxia) can also result in the high frequency of AOM. Likewise, the enhancement of water level has formed an oxygen minimum zone/environment in the proximal setting, resulting in high preservation of AOM. Moreover, the diversity of *Spinizonocolpites* (*Nypa* pollen) in the studied samples indicated the existence of mangrove vegetation in various brackish water habitats (Fredericksen 1994). Likewise, arthropod groups (midges and spiders in the present case) are found in abundance, native to shore areas of freshwater habitats, while a few species of family Chironomidae also indicate marine environment (Brodin and Andersson, 2009; Hodge and Vink, 2020) and offshore regions. Arachnids, however, are more confined to areas where there is easy access to prey and suitable modes for reproduction. Hence, a fluctuating water conditions (freshwater-brackish) and suboxic-anoxic settings can be deduced from this facies.

Distal-suboxic-anoxic basin, IX (Palynofacies zone-III; lithology: clay/claystone)—signified a high incidence of well-preserved AOM along with some non-biostructured, opaque phytoclast, fungal and cuticle elements. The granular type (principally) of AOM has been observed in this facies (fig. 6n). According to Pacton et al. (2011), the granular AOM is a product of microbial activity. It can also be noted that the concentration of AOM is generally enhanced towards the basinal (anoxic) settings (Dow and Pearson, 1975; Bujak et al., 1977). Subsequently, a relatively high incidence (mainly lath-shaped) of opaque phytoclast (more refractory) indicates distal (to source) settings (Mendonça Filho et al., 2014). Moreover, the occurrence of fungal elements indicates a warm and humid environmental condition at the depositional site. They digest the cellular structures that led to the degradation of OM (Peters et al., 2013). This facies is suggestive of distal settings with suboxic to anoxic conditions.

Thus, the overall characteristics suggest that lush angiosperm dominant forest vegetation composed of herbs, shrubs, woody forest and mangrove elements formed the source of Valia lignite deposits, and that were eventually deposited in a proximal setting under fluctuating environments (freshwater-brackish).

5.3. Hydrocarbon generation potential

The results of geochemical screening (Rock-Eval pyrolysis) have reliably been used in academic and industrial spheres for decades, particularly for the assessment of hydrocarbons plays. The technique is simple, inexpensive, required less sample amount, and generates reliable data (Lafargue et al., 1998). Several workers have presented many guidelines/critical observations to improve the

understanding of Rock-Eval data and eliminate misinterpretation (Sykes and Snowdon, 2002; Dembicki Jr., 2009; Carvajal-Ortiz and Gentzis, 2015; Hazra et al., 2021; and many others).

The measurement of TOC (in weight percentage), although OM also contains hydrogen, nitrogen, oxygen and sulphur, is considered as the most significant parameter to evaluate the quantity of OM. The amount of OM present in the sediment has been influenced by many factors, such as primary production, rate of sedimentation, the environment of deposition and the burial history of sediment. The sediment/rock containing >2 wt.% of TOC is considered as an excellent source for hydrocarbons (Peters, 1986; Peters and Cassa, 1994). In the studied samples, the TOC contents (35.90-55.60 wt.% in lignites, 12.20-16.20 wt.% in Carb. Shales, 1.46-2.83 wt.% in shales) suggesting a good to excellent potential for these organic-rich deposits to produce hydrocarbons. On the other hand, for the generation of hydrocarbons, the OM must have hydrogen associated with carbon (Dembicki Jr., 2009). The S₂ peak (of Rock-Eval) indicates the amount of hydrocarbons generation, and is usually higher for the OM with high liptinite macerals (H-rich). Hence, the combination of S₂ and TOC will provide useful insight into the hydrocarbon generation. The cross plot of S₂ values against TOC contents (Fig. 17a) indicates an excellent hydrocarbon potentiality of the Valia samples.

The inertinite macerals/opaque phytoclast/inert carbon contents also contribute to the TOC concentration, and play no role in the generation of hydrocarbons. Therefore, it is important to determine the types of OM (Dow, 1977; Tissot and Welte, 1984; Peters, 1986; Dembicki Jr., 2009). The HI [(S₂/TOC)*100] value >200 mg HC/gTOC is generally considered good for the generation of liquid hydrocarbons (Bordenave and Durand, 1993; Peters and Cassa, 1994, Hunt, 1996; Sykes and Snowdon, 2002). The plotting of calculated values of HI and OI [(S₃/TOC)*100] indicates that the studied samples contain an admixed type-III and II kerogen (Fig. 17b), and can generate mainly gaseous hydrocarbon. The high HI value of sample VA-47 could be assigned to the heterogeneity, vegetational influx and the preservation state of the OM. Alternatively, these 'abnormal' values can also be caused by the subtle environment change reflected by the high inorganic (mineral matter/Ash yield) contents and high GI and GWI values (Petersen et al., 2009). Similarly, the relationship between HI and TOC (Fig. 17c) also shows that these deposits have a fair potential to generate gaseous and some liquid hydrocarbons.

Further, the OM with good S₂ and TOC contents must be 'cooked' enough for the hydrocarbons production. Hence, the determination of thermal maturity is vital for the assessment of hydrocarbon exploration/prospect. The thermal maturation of OM is convincingly evaluated from the T_{max} (Rock-Eval pyrolysis) and vitrinite/huminite reflectance (organic petrography) parameters (Peters and Cassa, 1994; Taylor et al., 1998). However, precautions should be taken while using these parameters, as they

are influenced by various factors, such as OM types, depositional environments, etc. (Snowdon, 1995, Sykes and Snowdon, 2002, Dembicki Jr., 2009). The T_{max} values of Valia samples are generally low (below 435 °C). The cross plot of HI vs. T_{max} (Fig. 17d) indicates the immature nature of lignite and carbonaceous shale samples, while shale sediments fall at the edge of the immature-mature zone. According to Yang and Horsfield, (2020) various factors such as clay richness and oxidation or reworking can affect the T_{max} values. Similarly, the vitrinite/huminite reflectance is a robust method for depicting the thermal maturity in conventional and unconventional hydrocarbon systems (Hackley et al., 2015; and reference therein). The random reflectance values (0.26-0.30%) categorised the Valia lignites as low rank-C, thus indicates immature nature. The other parameter used here for determining the maturation is the atomic ratios of H/C and O/C on the van Krevelen diagram. The ratios indicate that the OM reached up the early diagenesis stage (immature) of coalification, and mainly contains type-III kerogen (Fig. 18). Likewise, the high values of OI and low values of production index [PI= $S_1/(S_1+S_2)$] also suggesting the immature nature of the studied sediments, and less chance for in-situ liquid hydrocarbon generation (Garcia-Vallés et al., 2000).

Additionally, the average values of volatile matter yields (58.61 wt.%), carbon contents (68.43 wt.%) and gross calorific values (4467 Cal/g), also indicating the immaturity of the studied deposits. The hop-17(21)-ene is present in majority of samples, that generally occurs in immature coal/lignite samples (Bechtel et al., 2003, 2005). The extended hopanes are also present in the samples. The presence of compounds with thermally unstable $\beta\beta$ -configuration points to the low degree of hopanoid alteration, and suggesting thermally immature nature of the OM (Petersen et al., 2004). Altogether, it is evident that the Valia lignite-bearing succession with having admixed type-III/II kerogen can generate gaseous and some liquid hydrocarbons upon maturation or with additional heating.

6. *Conclusions*

The integration of petrographical, palynofacies, palynological and geochemical parameters is significant to provide a comprehensive account of nature, composition, maturation, palaeoecology, depositional settings, and hydrocarbon generation potential of the Valia lignite deposits of Gujarat in western India. Remarkably, the entomological studies of the Cambay amber offer an opportunity to understand the existence of fauna (fossil arthropod) within the existing flora (forests), and open a window to learn more about the fascinating life forms of the past. This approach will have broad biological significance for identifying the ecological pattern of different biotic communities and their dispersal in the geological time. Based on the combined approach, this study obtains the following conclusions:

- The low rank-C lignites are chiefly composed of huminite group (mainly detrohuminites)/phytoclats OM. The lignites are characterised by high carbon contents and volatile matter yields, moderate fixed carbon contents and low ash yields.
- The maceral composition, palynofacies assemblage and biomarker data suggest that both land plants and macrophytes contribute significantly to the peat formation. The recovered palynomorphs and the pentacyclic non-hopanoid compounds with oleanane-type structures indicate that angiosperms were the main precursors of peat-forming vegetation.
- The limno-telmatic peat-forming vegetation was deposited under the back-barrier environment with fluctuating (mesotrophic to rheotrophic) hydrological settings.
- The occurrences and diversity of *Spinizonocolpites* (*Nypa*-pollen), framboidal pyrite, sulphur, and the high variability of ash yields are indicating a brackish environment. However, the abundance of insects' family Chironomidae and occurrences of pteridophytic spores like *Dictyophyllidites laevigatus*, *Todiosporites plicatus*, *Dandotiaspora dilate* together with maceral alginite (*Botryococcus*) indicate freshwater condition.
- The palynofacies assemblages suggests that the deposition of OM took place (mainly) under dysoxic-suboxic conditions in proximal settings. The Pr/Ph ratio and Pr/n-C₁₇ vs. Ph/n-C₁₈ plot are also indicating suboxic conditions.
- The relative abundances of hopanes, non-biostructured, gelified-AOM and detrohuminite indicate the exceeding level of biodegradation (bacterial activity) of the OM.
- The TOC contents, hydrogen-rich macerals (liptinite + perhydrous huminite) and HI values indicate that the studied deposits are of a good to excellent source of hydrocarbon generation. The atomic ratios of H/C and O/C and occurrences of $\beta\beta$ -hopane along with the values of R_r, T_{max}, GCV show the immature nature of the deposits.
- The relationship between different petro-geochemical parameters indicates that the lignite-bearing sequence of Valia mine contains admixed type-III/II kerogen, and capable of generating gaseous (mainly) and some liquid hydrocarbons through thermal cracking.

Acknowledgements

Authors are grateful to the Director, BSIP (Lucknow) for her constant encouragements, and for granting permission (BSIP/RDCC/02/2021-22) to publish this paper. We are thankful to the officials of Gujarat Industries Power Company Ltd. (Vadodara) and Valia Lignite Mine Project (Bharuch) for their help and supports. VPS is grateful to DST-SERB (Govt. of India) for providing the National Post-Doctoral Fellowship (PDF/2018/000883). KAS thank Director, ZSI (Kolkata) for encouragement and support.

We thank Dr. Cevat Özgen Karacan for the editorial support. We sincerely appreciate the reviewers for their constructive comments and valuable suggestions that helped us to improve the previous version of this article.

References

- Agnihotri, P., Singh, H., 2020. Eocene biodiversity of Eocene amber from the Umarsar Lignites, Kutch Basin, Gujarat- India. *J. Palaeontol. Soc. India*, 65(2), 214-218.
- Alimohammadian, H., Sahni, A., Patnaik, R., Rana, R.S., Singh, H., 2005. First record of an exceptionally diverse and well-preserved amber-embedded biota from lower Eocene (~53 Ma) lignites, Vastan, Gujarat. *Curr. Sci.*, 89: 1328-1330
- Andersson, R.A., Kuhry, P., Meyers, P., Zebühr, Y., Crill, P., Mörth, M., 2011. Impacts of paleohydrological changes on *n*-alkane biomarker compositions of a Holocene peat sequence in the eastern European Russian Arctic. *Org. Geochem.*, 42, 1065-1075.
- ASTM (American Society for Testing and Material), 1993. Standard Test Method for Sulphur in the Analysis Sample of Coal and Coke, D 3177-89, Annual Book of ASTM standards, Petroleum Products, Lubricants and Fossil Fuels, Vol. 05.05, Gaseous Fuels; Coal and Coke, Philadelphia, PA, pp. 306-309.
- ASTM (American Society for Testing and Material), 1993. Standard Test Method for Carbon and Hydrogen in the Analysis Sample of Coal and Coke, D 3178-89, Annual Book of ASTM standards, Petroleum Products, Lubricants and Fossil Fuels, vol. 05.05, Gaseous Fuels; Coal and Coke, Philadelphia, PA, pp. 310-313.
- ASTM (American Society for Testing and Material), 1993. Standard Test Method for Nitrogen in the Analysis Sample of Coal and Coke, D 3179, Annual Book of ASTM standards, Petroleum Products, Lubricants and Fossil Fuels, vol. 05.05, Gaseous Fuels; Coal and Coke, ASTM, Philadelphia, PA, pp. 314-318.
- ASTM (American Society for Testing and Material), 1996. Standard Test Method for Gross Calorific Value of Solid Fuel by the Adiabatic Bomb Calorimeter, ASTM D2015.
- Bajpai, S., Kapur, V.V., 2004. Oldest known gobiids from Vastan Lignite Mine (early Eocene). Surat District, Gujarat. *Curr. Sci.*, 87, 433-435.
- Bajpai, S., Kapur, V.V., Thewissen, J.G.M., Das, D.P., Tiwari, B.N., 2006. New early Eocene Cambaythere (Perrisodactyla, Mammalia) from the Vastan lignite mine (Gujarat, India) and an evaluation of Cambaythere relationships. *J. Palaeontol. Soc. India*, 51, 101-110.
- Baker, A., Routh, J., Roychoudhury, A.N., 2016. Biomarker records of palaeoenvironmental variations in subtropical Southern Africa since the late Pleistocene: Evidences from a coastal peatland. *Palaeogeogr., Palaeoclimatol., Palaeoecol.*, 451, 1-12.
- Batten, D.J., Stead, D.T., 2005. Palynofacies analysis and its stratigraphic application. In: Koutsoukos, E.A.M. (Ed.), *Applied Stratigraphy*. Springer, Dordrecht, Netherlands, pp. 203-226.

- Bechtel, A., Gruber, W., Sachsenhofer, R.F., Gratzner, R., Lucke, A., Puttmann, W., 2003. Depositional environment of the Late Miocene Hausruck lignite (Alpine Foreland Basin); insights from petrography, organic geochemistry and stable carbon isotopes, *Int. J. Coal Geol.*, 53, 153-180,
- Bechtel, A., Gruber, W., Sachsenhofer, R.F., Gratzner, R., Püttmann, W., 2001. Organic geochemical and stable isotopic investigation of coals formed in low-lying and raised mires within the Eastern Alps (Austria). *Org. Geochem.*, 32, 1289-1310.
- Bechtel, A., Sachsenhofer, R.F., Zdravkov, A., Kostova, I., Gratzner, R., 2005. Influence of floral assemblage, facies and diagenesis on petrography and organic geochemistry of the Eocene Bourgas coal and the Miocene Maritza-East lignite (Bulgaria). *Org. Geochem.*, 36, 1498-1522.
- Bhandari, A., Singh, H., Rana, R.S., 2005. A note on the occurrence of Ostracoda from the Vastan Lignite Mine, Gujarat. *J. Palaeontol. Soc. India*, 50, 141-146.
- BIS (Bureau of Indian Standard), 2003. Methods of Test for Coal and Coke (2nd revision of IS: 1350). Part I, Proximate analysis. Bureau of Indian Standard, New Delhi, pp. 1-29.
- Biswas, S.K., 1982. Rift basins in western margin of India and their hydrocarbon prospects with special reference to Kutch Basin. *AAPG Bull.*, 65, 1497-1513.
- Biswas, S.K., 1987. Regional tectonic framework, structure and evolution of the western marginal basins of India. *Tectonophysics*, 135, 307-327.
- Biswas, S.K., 1999. Review of the evolution of the rift basins in India during Gondwana with special reference to western Indian basins and their hydrocarbon prospective. *Proc. Natl. Acad. Sci.*, 65, 226-238.
- Bordenave, M.L., Durand, B., 1993. Evolution of ideas and concepts in geochemistry. In: Bordenave, M.L. (Ed.), *Applied Petroleum Geochemistry*. Editions Technip, pp. 5-14.
- Bourbonniere, R.A., Meyers, P.A., 1996. Sedimentary geolipid records of historical changes in the watersheds and productivities of Lakes Ontario and Erie. *Limnol. and Oceanogr.*, 41, 352-359.
- Bray, E., Evans, E., 1961. Distribution of *n*-paraffins as a clue to recognition of source beds. *Geochim. Cosmochim. Acta*, 22, 2-15.
- Brodin, Y., Andersson, M.H., 2009. The marine splash midge *Telmatogon japonicus* (Diptera; Chironomidae) – extreme and alien? *Springer*, 11, 1311-1317.
- Bujak, J.P., Barss, M.S., Williams, G.L., 1977. Offshore east Canada's organic type and color and hydrocarbon potential. *The Oil and Gas J.*, 75, 198-201.
- Calder, J.H., Gibbing, M.R., Mukhopadhyay, P.K., 1991. Peat formation in a Westphalian B piedmont setting, Cumberland Basin, Nova Scotia: implication for the maceral-based interpretation of rheotrophic and raised paleomires. *Bull. Soc. Geol. Fr.*, 162, 283-298.
- Caldicott, A.B., Eglinton, G., 1973. Surface waxes. In: Miller, L.P., (Ed.), *Phytochemistry*, Vol. III. van Nostrand Reinhold, New York.
- Carvajal-Ortiz, H., Gentzis, T., 2015. Critical considerations when assessing hydrocarbon plays using Rock-Eval pyrolysis and organic petrology data: data quality revisited. *Int. J. Coal Geol.*, 152, 113-122

- Chandra, P.K., Chowdhary, L.R., 1969. Stratigraphy of Cambay Basin. *Bull. ONGC*, 6(2), 37-50.
- Clementz, M., Bajpai, S., Ravikant, V., Thewissen, J.G.M., Saravanan, N., Singh, I.B., Prasad, V., 2011. Early Eocene warming events and the timing of terrestrial faunal exchange between India and Asia. *Geology*, 39, 15-18.
- Crosdale, P.J., 1993. Coal maceral ratios as indicators of environment of deposition: do they work for ombrogenous mires? *Org. Geochem.*, 20, 997-809.
- Dehmer, J., 1995. Petrological and organic geochemical investigation of recent peats with known environments of deposition. *Int. J. Coal Geol.*, 28 (2-4), 111-138.
- Dembicki Jr., H., 2009. Three common source rock evaluation errors made by geologists during prospect or play appraisals. *AAPG Bull.*, 93, 341-356.
- Dickens, G.R., O'Neil, J.R., Rea, D.K., Owen, R.M., 1995. Dissociation of oceanic methane hydrate as a cause of the carbon isotope excursion at the end of the Paleocene. *Paleoceanography*, 10(6), 965-971.
- Didyk, B.M., Simoneit, B.R.T., Brassell, S.C., Eglinton, G., 1978. Organic geochemical indicators of paleoenvironmental conditions of sedimentation. *Nature*, 272, 216-222.
- Diessel, C.F.K., 1986. On the correlation between coal facies and depositional environments. *Proc. 20th Newcastle Symp. The University of Newcastle*, pp. 19-22.
- Diessel, C.F.K., 1992. *Coal-bearing Depositional Systems*. Springer-Verlag, Berlin.
- Dilcher, D.L., 1965. Epiphyllous fungi from Eocene deposits in western Tennessee, USA. *Palaeontog. B*, 116, 1-54.
- Dow, W.G., 1977. Kerogen studies and geological interpretations. *J. Geochem. Explor.*, 7, 79-99.
- Dow, W.G., Pearson, D.B., 1975. Organic matter in Gulf coast sediments. In: *Reprints, Seventh Annual Offshore Technology Conference. Offshore Technol. Conf.*, pp. 85-90.
- Dransfield, J., Uhl, N.W., Asmussen, C.B., Baker, W.J., Harley, M.M., Lewis, C.B., 2008. *Genera Palmarum: The Evolution and Classification of Palms*. Royal Botanic Gardens Kew, pp. 732.
- Dutta, S., Kumar, S., Singh, H., Khan, M.A., Barai, A., Tewari, A., Rana, R.S., Bera, S., Sen, S., Sahni, A., 2020. Chemical Evidence of Preserved Collagenin 54-Million-Year-Old Fish Vertebrae. *Palaeontology*, 63(2), 1-8.
- Dutta, S., Mallick, M., Bertram, N., Greenwood, P.F., Mathews, R.P., 2009. Terpenoid composition and class of Tertiary resins from India. *Int. J. Coal Geol.*, 80, 44-50.
- Dutta, S., Mallick, M., Kumar, K., Mann, U., Greenwood, P.F., 2011b. Terpenoid composition and botanical affinity of cretaceous resins from India and Myanmar. *Int. J. Coal Geol.* 85, 49–55.
- Dutta, S., Mathews, R.P., Singh, B.D., Tripathi, S.K.M., Singh, A., Saraswati, P.K., Banerjee, S., Mann, U., 2011a. Petrology, palynology and organic geochemistry of Eocene lignite of Matanomadh, Kutch Basin, western India: implications to depositional environment and hydrocarbon source potential. *Int. J. Coal Geol.*, 85, 91-102.

- Edwards, W.N., 1922. An Eocene microthyriaceous fungus from Mull, Scotland. *Trans. British Mycolog. Soc.*, 8, 66-72.
- Eglinton, G., Hamilton, R.J., 1967. Leaf epicuticular waxes. *Science*, 156, 1322-1335.
- Engel, M.S., Grimaldi, D.A., Nascimbene, P.C., Singh, H., 2011. The termites of Early Eocene Cambay amber, with the earliest record of the Termitidae (Isoptera). *Zookeys*, 105.
- Espitalié J., Deroo, G., Marquis, F., 1985. La pyrolyse Rock-Eval et ses applications (part I). *Rev. Inst. Fr. Pet.*, 40, 563–579.
- Ficken, K.J., Li, B., Swain, D.L., Eglinton, G., 2000. An *n*-alkane proxy for the sedimentary input of submerged/floating freshwater aquatic macrophytes. *Org. Geochem.*, 31, 745-749.
- Folie, A., Rana, R.S., Rose, K.D., Sahni, A., Kumar, K., Singh, L., Smith, T., 2013. Early Eocene frogs from Vastan Lignite Mine, Gujarat, India. *Acta Palaeont. Polo.*, 58(3), 511-524.
- Frederiksen, N.O., 1994. Middle and late Palaeocene angiosperm pollen from Pakistan. *Palynology*, 18, 91-137.
- Garcia-Vallés, M., Vendrell-Saz, M., Pradell-Cara, T., 2000. Organic geochemistry (Rock-Eval) and maturation rank of the Garumnian coal in the Central Pyrenees (Spain). *Fuel*, 79, 505-513.
- Garg, R., Ateequzaman, K., Prasad, V., Tripathi, S.K.M., Singh, I.B., Jauhri, A.K., Bajpai, S., 2008. Age-diagnostic dinoflagellate cysts from the lignite bearing sediments of the Vastan lignite mine, Surat District, Gujarat, western India. *J. Palaeontol. Soc. India*, 53 (1), 99-105.
- Gelpi, E., Schneider, H., Mann, J., Oro, J., 1970. Hydrocarbons of geochemical significance in microscopic algae. *Phytochem.*, 9, 603-612.
- Greenwood, D.R., Wing, S.L., 1995. Eocene continental climates and latitudinal temperature gradients. *Geology*, 23(11), 1044-1048.
- Grimaldi, D., Singh, H., 2012. The extinct genus *Pareuthychaeta* in Eocene ambers (Diptera: Schizophora: Ephydroidea). *The Can. Entom.*, 144 (1), 17-28.
- Hackley, P.C., Araujo, C.V., Borrego, A.G., Bouzinos, A., Cardott, B.J., Cook, A.C., Eble, C., Flores, D., Gentzis, T., Gonçalves, P.A., Mendonça Filho, J.G., Hamor-Vid, M., Jelonek, I., Kommeren, K., Knowles, W., Kus, J., Mastalerz, M., Menezes, T.R., Newman, J., Oikonomopoulos, I.K., Pawlewicz, M., Pickel, W., Potter, J., Ranasinghe, P., Read, H., Reyes, J., Rodriguez, G. De La R., de Souza, I.V.A.F., Suarez-Ruiz, I., Sýkorova, I., Valentine, B.J., 2015. Standardization of reflectance measurements in dispersed organic matter: Results of an exercise to improve interlaboratory agreement. *J. Mar. Pet. Geol.*, 59, 22-34
- Haq, B.U., Hardenbol, J., Vail, P.R., 1987. Chronology of fluctuating sea levels since the Triassic. *Science*, 235, 1156-1167
- Harms, D., Dunlop, J.A., 2017. The fossil history of pseudoscorpions (Arachnida: Pseudoscorpiones). *Fossil Record*, 20, 215-238.
- Hazra, B., Singh, D.P., Crossdale, P.J., Singh, V., Singh, P.K., Gangopadhyay, M., Chakraborty, P., 2021. Critical insight from Rock-Eval analysis of vitrains. *Int. J. Coal Geol.*, 238, 103717.

- Hodge, S., Vink, C., 2020. The prevalence and species richness of spiders associated with marine strandlines on different shore types around Banks Peninsula, New Zealand. *New Zealand J. Zoo.*, 47, 71-85.
- Horne, D.J., 2005. Ostracoda. In: *Encyclopaedia of geology*. Oxford, UK: Elsevier. (3), pp. 453–463.
- Hunt, J.M., 1996. *Petroleum Geochemistry and Geology* (2nd edition). Freeman, New York.
- ICCP, 2001. The new inertinite classification (ICCP System 1994), International Committee for Coal and Organic Petrology. *Fuel*, 80, 459-471.
- ISO 7404-2, 2009. *Methods for the Petrographic Analysis of Bituminous Coal and Anthracite— Part 2: Methods of Preparing Coal Samples*. International Organization for Standardization, ISO, Geneva, pp. 8.
- ISO 7404-3, 2009. *Methods for the Petrographic Analysis of Bituminous Coal and Anthracite— Part 3: Methods of Determining Maceral Group Composition*. International Organization for Standardization, ISO, Geneva, pp. 4.
- ISO 7404-5, 2009. *Methods for the Petrographic Analysis of Bituminous Coal and Anthracite— Part 5: Methods of Determining Microscopically the Reflectance of Vitrinite*. International Organization for Standardization, ISO, Geneva, pp. 11.
- ISO-11760, 2005. *Classification of Coals*. International Standard, pp. 1-9.
- Jain, K.P., Kar, R.K., Sah, S.C.D., 1973. A palynological assemblage from Barmer, Rajasthan. *Geophytology*, 3(2), 150-165.
- Kalaitzidis S., Bouzinos, A., Papazisimou, S., Christanis, K., 2004. A short-term establishment of forest fen habitat during Pliocene lignite formation in the Ptolemais Basin, NW Macedonia, Greece. *Int. J. Coal Geol.*, 57, 243-263.
- Kalkreuth, W., Holz, M., Mexias, A., Balbinot, M., Levandowski, J., Willett, J., Finkelman, R., Burger, H., 2010. Depositional setting, petrology and chemistry of Permian coals from the Paraná Basin: 2. South Santa Catarina Coalfield, Brazil. *Int. J. Coal Geol.*, 84, 213-236.
- Kalkreuth, W., Kotis, T., Papanikolaou, C., Kokkinakis, P., 1991. The geology and coal petrology of a Miocene lignite profile at Meliadi Mine, Katerini, Greece. *Int. J. Coal Geol.*, 17, 51-67.
- Kania, I., Krzemiński, W., Stebner, F., Singh, H., 2017. The first representative of Tipulomorpha (Diptera) from Early Eocene Cambay amber (India). *Earth Env. Sci. Trans. Royal Soc. Edinburgh*, 107(2-3), 263-269.
- Kar, R.K., 1985. The fossil floras of Kachchh. IV- Tertiary Palynostratigraphy. *Palaeobotanist*, 34, 1-279.
- Karrer, W., Cherbuliez, E., Eugster, C.H., 1977. *Konstitution und vorkommen der organischen Pflanzenstoffe (exclusive Alkaloide) Ergänzungsband, vol. 1*. Birkhäuser Verlag, Basel.
- Kennett, J.P., Stott, L., 1991. Abrupt deep sea warming, paleoceanographic changes and benthic extinctions at the end of the Paleocene. *Nature*, 353, 319-322.

- Kocsis, L., Usman, A., Jourdan, Anne-L., Hassan, Syaimaa' H., Jumat, N. Daud, D., Briguglio, A., Slik, F., Rinyu, L., Futo, I., 2020. The Bruneian record of "Borneo Amber": A regional review of fossil tree resins in the Indo-Australian Archipelago. *Earth-Sci. Rev.* 201, 103005.
- Krishnan, M.S., 1968. *Geology of India and Burma*, Higginbothams, Madras.
- Lafargue, E., Marquis, F., Pillot, D., 1998. Rock-Eval-6 applications in hydrocarbon exploration, production and soil contamination studies. *Oil Gas Sci. Technol.*, 53, 421-437.
- Mallick, M., Dutta, S., Greenwood, P.F., 2014. Molecular characterization of fossil and extant dammar resin extracts: Insights into diagenetic fate of sesqui- and triterpenoids. *Int. J. Coal Geol.* 121, 129–136.
- Mallick, M., Dutta, S., Greenwood, P.F., Bertram, N., 2009. Pyrolytic and spectroscopic studies of Eocene resin from Vastan Lignite Mine, Cambay Basin, western India. *J. Geol. Soc. India*, 74(1), 16-22.
- Mallick, M., Dutta, S., Singh, B.D., Bhattacharya, S., Singh, A., 2021. Petrographic and organic geochemical characterizations of Early Eocene lignites, Cambay Basin, Western India. In: Bhui U.K. (Ed.) *Macromolecular Characterization of Hydrocarbons for Sustainable Future, Green Energy and Technology*, Springer, pp. 143-171.
- Mandal, J., Guleria, J.S., 2006. Palynology of Vastan Lignite (Surat District), Gujarat, its age, palaeoecology and depositional environment. *Palaeobotanist*, 55, 51-66.
- Mathews, R.P., Chetia, R., Agrawal, S., Singh, B.D., Singh, P.K., Singh, V.P., Singh, A., 2020b. Early Palaeogene climate variability based on *n*-alkane and stable carbon isotopic composition evidenced from the Barsingsar lignite-bearing sequence of Rajasthan. *J. Geol. Soc. India*, 95, 255-262
- Mathews, R.P., Singh, B.D., Singh, V.P., Singh, A., Singh, H., Mahesh, S, Dutta, S., Mendhe, V.A., Chetia, R., 2020a. Organo-petrographic and geochemical characteristics of Gurha lignite deposits, Rajasthan, India: Insights into the palaeovegetation, palaeoenvironment and hydrocarbon source rock potential. *Geosci. Front.*, 11, 965-988.
- Mathur, L.P., Rao, K.L.N., Chaube, A.N., 1968. Tectonic framework of Cambay Basin, India. *Bull. ONGC*, 5(1).
- Mayr, G., Rana, R.S., Rose, K.D., Sahni, A., Kumar, K., Singh, L., Smith, T., 2010. Quercypsitta-Like Birds from the early Eocene of India (Aves, ?Psittaciformes). *J. Vert. Paleont.* 30(2), 467-478.
- Mendonça Filho, J.G., Carvalho, M.A., Menezes, T.R., 2002. Palinofácies. In: Dutra, T.L. (Ed.), *Técnicas e Procedimentos para o Trabalho com Fósseis e Formas Modernas Comparativas*. Unisinos, São Leopoldo, pp. 20-24.
- Mendonça Filho, J.G., Menezes, T.R., Mendonça, J.O., 2011. Organic composition (palynofacies analysis). Chapter 5, *ICCP Training Course on Dispersed Organic Matter*, pp. 33-81.
- Mendonça Filho, J.G., Menezes, T.R., Mendonça, J.O., 2014. Trends in Kerogen Groups Distribution, Training course on Dispersed Organic Matter (DOM). (Unpublished study material).
- Merh, S.S., 1995. *Geology of Gujarat*. Geological Society of India, Bangalore.

- Moore, T.A., Shearer, J.C., 2003. Peat/coal type and depositional environment- are they related? *Int. J. Coal Geol.*, 56, 233-252.
- Morley, R.J., 2000. *Origin and evolution of tropical rain forest*. John Wiley & Sons Ltd.
- Morley, R.J., 2003. Interplate dispersal paths for megathermal angiosperms. *Persp. Plant Ecol., Evol. Syst.*, 6(1,2), 5-20.
- Naglik, B., Kosmowska-Ceranawicz, B., Natkaniec-Nowak, L., Drzewicz, P., Dumanska-Slowik, M., Matusik, J., Wagner, M., Milovsky, R., Stach, P., Szyszka, A., 2018. Fossilization History of Fossil Resin from Jambi Province (Sumatra, Indonesia) Based on Physico-Chemical Studies. *Minerals*, 8, 95.
- Nagori, M.L., Khosla, S.C., Jakhar, S.R., 2013. Middle Eocene Ostracoda from the Tadkeshwar Lignite Mine, Cambay Basin, Gujarat. *J. Geol. Soc. India*, 81, 514-520.
- Nascimbene, P.C., Silverstein, H., 2000. The preparation of fragile Cretaceous ambers for conservation and study of organismal inclusions. In: Grimaldi, D., (Ed.) *Studies on fossils in amber, with particular reference to the Cretaceous of New Jersey*. Backhuys, Leiden. pp. 93-102.
- Noble, R.A., Alexander, R., Kagi, R.I., Knox, J., 1985. Tetracyclic diterpenoid hydrocarbons in some Australian coals, sediments and crude oils, *Geochim. Cosmochim. Acta*, 49, 2141–2147.
- Nolf, D., Rana, R.S., Singh, H., 2006. Fish otoliths from the Ypresian (early Eocene) of Vastan, Gujarat, India. *Bull. Inst. R. Sci. Nat. Belg. Sci. Terre*, 76, 105-118.
- Nott, C.J., Xie, S., Avsejs, L.A., Maddy, D., Chambers, F.M., Evershed, R.P., 2000. *n*-Alkane distributions in ombrotrophic mires as indicators of vegetation change related to climatic variation. *Org. Geochem.*, 31, 231-235.
- Ortega-Blanco, J., Chatzimanolis, S., Singh, H., Engel, M.S., 2013. The oldest fossil of the subfamily Osoriinae (Coleoptera: Staphylinidae), from Eocene Cambay amber (India). *The Coleop. Bull.*, 67(3): 304-308.
- Otto, A., Walther, H., Püttmann, W., 1994. Molecular composition of a leaf- and root-bearing Oligocene Oxbow Lake Clay in the Weissenster Basin, Germany. *Org. Geochem.*, 22(2), 275-286.
- Ourisson, G., Albrecht, P., Rohmer, M., 1979. The hopanoids. *Pure Appl. Chem.*, 51, 709-729.
- Pacton, M., Gorin, G.E., Vasconcelos, C., 2011. Amorphous organic matter— experimental data on formation and the role of microbes. *Rev. Palaeobot. Palynol.*, 166, 253-267.
- Pandey, J., Singh, N.P., Krishna, B.R., Sharma, D.D., Paraiikh, A.K., Nath, S.S., 1993. *Lithostratigraphy of Indian Petroliferous Basins Document-III, Cambay Basin*, KDM Institute of Petroleum Exploration ONGC, Dehradun, 1-166.
- Paul, S., Sharma, J., Singh, B.D., Saraswati, P.K., Dutta S., 2015. Early Eocene equatorial vegetation and depositional environment: Biomarker and palynological evidences from a lignite-bearing sequence of Cambay Basin, western India. *Int. J. Coal Geol.*, 149, 77-92.

- Peters, A.D., Agama, C.I., Asiedu, D.K., Apesegah, E., 2013. Palynology, palynofacies and Palaeoenvironments of sedimentary organic matter from Bonyere - 1 well, Tanobasin, western Ghana. *Int. Lett. Nat. Sci.*, 5, 27-45.
- Peters, K.E., 1986. Guidelines for evaluating petroleum source rock using programmed pyrolysis. *AAPG Bull.*, 70, 318-386.
- Peters, K.E., Cassa M.R., 1994. Applied source rock geochemistry. In: Magoon, L.B., Dow, W.G. (Eds.), *The Petroleum System from Source to Trap*, AAPG Mem., 60, 93-120.
- Peters, K.E., Moldowan, J.M., 1993. *The biomarker guide: interpreting molecular fossils in petroleum and ancient sediments*. Prentice Hall, NJ, USA.
- Peters, K.E., Walters, C.C., Moldowan, J.M., 2005. *The Biomarker Guide*. Cambridge University, New York.
- Petersen, H.I., Lindström, S., Nytoft, H.P., Rosenberg, P., 2009. Composition, peat-forming vegetation and kerogen paraffinicity of Cenozoic coals: Relationship to variations in the petroleum generation potential (Hydrogen Index). *Int. J Coal Geol.*, 78, 119-134.
- Petersen, H.I., Nytoft, H.P., Nielsen, L.H., 2004. Characterisation of oil and potential source rocks in the north-eastern Song Hong Basin, Vietnam: Indications of a lacustrine-coal sourced petroleum system. *Org. Geochem.*, 35, 493-515.
- Pickel, W., Kus, J., Flores, D., Kalaitzidis, S., Christanis, K., Cardott, B.J., Misz-Kennan, M., Rodrigues, S., Hentschel, A., Hamor-Vido, M., Crosdale, P., Wagner, N., ICCP, 2017. Classification of liptinite – ICCP System 1994. *Int. J. Coal Geol.*, 169, 40-61.
- Prasad, G.V.R., Bajpai, S., 2008. Agamid lizards from the early Eocene of western India: oldest Cenozoic lizards from South Asia. *Palaeont. Elect.* 11(1): 4a, 1-19.
- Prasad, M., Singh, H., Singh, S.K., 2014. Early Eocene *Annona* fossils from Vastan lignite Mine, Surat district, Gujarat, India: age, origin and palaeogeographic significance. *Curr. Sci.*, 107(10), 1730-1735.
- Prasad, V., Singh, I.B., Bajpai, S., Garg, R., Thakur, B., Singh, A., Saravanan, N., Kapur, V.V., 2013. Palynofacies and sedimentology-based high-resolution sequence stratigraphy of the lignite-bearing muddy coastal deposits (early Eocene) in the Vastan Lignite Mine, Gulf of Cambay, India. *Facies*, 59, 737-761.
- Punekar, J., Saraswati, P.K., 2010. Age of the Vastan lignite in context of some oldest Cenozoic fossil mammals from India. *J. Geol. Soc. India*, 76, 49-72.
- Qin, S., Sun, Y., Tang, Y., 2010. Long-term, low temperature simulation of early diagenetic alterations of organic matter from conifers: Aliphatic hydrocarbons. *Geochem. J.*, 44, 247-259.
- Radhwani, M., Bechtel, A., Singh, V.P., Singh, B.D., Mannai-Tayeche, B., 2018. Petrographic, palynofacies and geochemical characteristics of organic matter in the Saouef Formation (NE Tunisia): Origin, palaeoenvironment, and economic significance. *Int. J. Coal Geol.*, 187, 114-130.
- Rage, J.C., Folie, A., Rana, R.S., Singh, H., Rose, K.D., Smith, T., 2008. A diverse snake fauna from the early Eocene of Vastan Lignite Mine, at Gujarat, India. *Acta Palaeont. Polo.*, 53, 391-403.

- Raju, A.T.R., Srinivasan, S., 1983. More hydrocarbon from well explored Cambay Basin. *Petr. Asia J.* VI(4), 25-37.
- Ramanujam, C.G.K., 1995. Pteridophytes during the Tertiary period of south India as revealed by their characteristic sporomorphs. *Palaeobotanist*, 44, 152-156.
- Rana, R.S., Augé, M., Folie, A., Rose, K.D., Kumar, K., Singh, L., Sahni, A., Smith, T., 2013. High diversity of acrodontan lizards in the Early Eocene Vastan Lignite Mine of India. *Geol. Belg.*, 16/4, 290-301.
- Rana, R.S., Kumar, K., Escarguel, G., Sahni, A., Rose, K.D., Smith, T., Singh, H., Singh, L., 2008. An ailuravine rodent from the lower Eocene Cambay Formation at Vastan, western India and its palaeobiogeographic implications. *Acta Palaeont. Polo.*, 53, 1-14.
- Rana, R.S., Kumar, K., Singh, H., 2004. Vertebrate fauna from the subsurface Cambay shale (Lower Eocene), Vastan Lignite Mine, Gujarat, India, *Curr. Sci.*, 87, 1726-1733.
- Rana, R.S., Kumar, K., Singh, H., Rose, K.D., 2005. Lower vertebrates from the late Palaeocene-earliest Eocene Akli Formation Giral Lignite Mine Barmer District western India. *Curr. Sci.*, 89, 1606-1613.
- Rao, M.R., 1995. Palaeoecological and stratigraphical significance of pteridophytic spores in the Kerala Basin. *The Indian Fern J.*, 12, 97-104.
- Rao, M.R., Sahni, A., Rana, R.S., Verma, P., 2013. Palynostratigraphy and depositional environment of Vastan Lignite Mine (Early Eocene), Gujarat, western India. *J. Earth Syst. Sci.*, 122(2), 289-307.
- Rohmer, M., Bisseret, P., Neunlist, S., 1992. The hopanoids, procaryotic triterpenoids and precursors of ubiquitous molecular fossils. In: Moldowan, J.M. (Ed.), *Biological Markers in Sediments and Petroleum*. Prentice Hall, Englewood Cliffs, New Jersey, pp. 1-17.
- Rose, K.D., Holbrook, L.T., Rana, R.S., Kumar, K., Jones, K.E., Ahrens, H.E., Missian, P., Sahni, A., Smith, T., 2014. Early Eocene fossils suggest that the mammalian order *Perrissodactyla* originated in India. *Nature Comm.*, 5, 55-70.
- Rose, K.D., Kumar, K., Rana, R.S., Sahni, A., Smith, T., 2013. New hypsodont tillodont (Mammalia, Tillodontia) from the Early Eocene of India. *J. Paleontol.*, 87(5), 842-853.
- Rose, K.D., Rana, R.S., Sahni, A., Kumar, K., Missiaen, P., Singh, L., Smith, T., 2009. Early Eocene primates from Gujarat, India. *J. Human Evol.*, 56, 366-404.
- Rose, K.D., Smith, T., Rana, R.S., Sahni, A., Singh, H., Missiaen, P., Folie, A., 2006. Early Eocene (Ypresian) continental vertebrate assemblage from India, with description of a new anthracobunid (Mammalia, Tethytheria). *J. Vertebr. Paleontol.*, 26, 219-225.
- Roy, T.K., 1990. Structural styles in Southern Cambay Basin. *Bull. ONGC*, 27(1), 15-56.
- Rust, J., Singh, H., Rana, R.S., McCann, T., Singh, U., Anderson, K., Sarkar, N., Nascimbene, P.C., Stebner, F., Thomas, J.C., Kraemer, M.S., Williams, C.J., Engel, M.S., Sahni, A., Grimaldi, D., 2010. Biogeographic and evolutionary implications of a diverse paleobiota in amber from the early Eocene of India. *Proc. Natl. Acad. Sci.*, 107 (43), 18360-18365.

- Sah, S.C.D., Kar, R.K., 1969. Pteridophytic spores from the Laki Series of Kutch, Gujarat, India. *J. Sen. Mem.*, 109-121.
- Sah, S.C.D., Kar, R.K., 1970. Palynology of the Laki sediments in Kutch: 3. Pollen from the bore holes around Jhulrai, Baranda and Panandhro. *Palaeobotanist*, 18(2), 127-142.
- Sahni A., Rana, R.S., Loyal, R.S., Saraswati, P.K., Mathur, S.K., Rose, K.D., Tripathi, S.K.M., Garg, R., 2004. Western margin Palaeocene–Lower Eocene lignites: Biostratigraphic and palaeoecological constraints. *Pro. 2nd Conf. Asso. Petro. Geol. ONGC*, 1-22.
- Sahni, A., Saraswati, P.K., Rana, R.S., Kumar, K., Singh, H., Alimohmmadian, H., Sahni, N., Rose, K.D., Singh, L., Smith, T., 2006. Temporal constraints and depositional environments of the Vastan lignite sequence, Gujarat: analogy for the Cambay Shale hydrocarbon source rock. *J. Petrol. Geol.*, 15, 1-20.
- Samant, B., Bajpai, S., 2001. Fish otoliths from the subsurface Cambay Shale (Lower Eocene), Surat Lignite Field, Gujarat (India). *Curr. Sci.*, 81(7), 758-759.
- Samant, B., Phadtare, N.R., 1997. Stratigraphic palynoflora of the Early Eocene Rajpardi lignite, Gujarat and the lower age limit of the Tarkeshwar Formation of South Cambay Basin, India. *Palaeonto. Abt. B*, 245 (1-6), 1-108.
- Samant, B., Tapaswi, P.M., 2000. Fungal remains from Surat Lignite deposits (EarlyEocene) of Gujarat, India, *Gond. Geol. Mag.*, 15, 25-30,
- Saxena, R.K., 1978. Palynology of the Matanomadh Formation in type area, north-western Kutch, India (Part I). Systematic description of pteridophytic spores. *Palaeobotanist*, 25, 448-456.
- Saxena, R.K., 1979. Reworked Cretaceous spores and pollen grains from the Matanomadh Formation (Palaeocene), Kutch, India. *Palaeobotanist*, 26(2), 167-174.
- Saxena, R.K., Khare, R.K., 2004. Palynological investigation of the Jayamkondacholapuram Well 12, Tiruchirapalli District, Tamil Nadu, India. *Geophytology*, 34(1-2), 73-93.
- Saxena, R.K., Tripathi, S.K.M., 2011. Indian Fossil Fungi. *Palaeobotanist*, 60, 1-208.
- Scotese, C.P., Golanka, J., 1992. Paleogeographic atlas, PALEOMAP progress report 20-0692. University of Texas, Arlington, 34.
- Scott, A.C., 2002. Coal petrology and the origin of coal macerals: a way ahead? *Int. J. Coal Geol.*, 50, 119-134.
- Selden, P.A., Penney, D., 2009. A fossil spider (Araneae: Pisauridae) of Eocene age from Horsefly, British Columbia, Canada. In *Towards a natural history of arthropods and other organisms*. In: Kropf, C., Horak, P., (Eds.) *memoriam Konrad Thaler Contributions to Natural History*, 12.
- Selkirk, D.R., 1975. Tertiary fossil fungi from Kiandra, New South Wales. *Proc. Linn. Soc. New South Wales* 100, 70-94.
- Shukla, A., Mehrotra, R.C., Guleria, J.S., 2013. Emergence and extinction of Dipterozooecia in western India with reference to climate change: fossil wood evidences. *J. Earth Syst. Sci.*, 122, 1373-1386.

- Shukla, A., Singh, H., Mehrotra, R.C., 2015. A fossil wood of *Gynocardia* from the Valia Lignite Mine, Bharuch District, Gujarat. *Palaeobotanist*, 64, 163-168.
- Silva, M.B., Kalkreuth, W., Holz, M., 2008. Coal petrology of coal seams from the Leão-Butiá Coalfield, Lower Permian of the Paraná Basin, Brazil: implications for coal facies interpretations. *Int. J. Coal Geol.*, 73, 331-358.
- Simoneit, B.R.T., Grimalt, J.O., Wang, T.G., Cox, R.E., Hatcher, P.G., Nissenbaum, A., 1986. Cyclic terpenoids of contemporary resinous plant detritus and fossil woods, ambers and coals. *Org. Geochem.* 10, 877–889.
- Simoneit, B.R.T., Oros, D. R., Karwowski, L., Szendera, L., Smolarek-Lach J., Goryl, M., Bucha, M., Rybicki, M., Marynowski, L. 2020. Terpenoid biomarkers of ambers from Miocene tropical paleoenvironments in Borneo and of their potential extant plant sources. *International Journal of Coal Geology*. 221, 103430.
- Simoneit, B.R.T., Otto, A., Kusumoto, N., Basinger, J.F., 2016. Biomarker compositions of *Glyptostrobus* and *Metasequoia* (Cupressaceae) fossils from the Eocene Buchanan Lake Formation, Axel Heiberg Island, Nunavut, Canada reflect diagenesis from terpenoids of their related extant species. *Rev. Palaeobot. Palynol.* 235, 81–93.
- Singh, A., Mahesh, S., Singh, H., Tripathi, S.K.M., Singh, B.D., 2013. Characterization of Mangrol lignite (Gujarat), India: Petrography, palynology, and palynofacies. *Int. J. Coal Geol.*, 120, 82-94.
- Singh, A., Shivanna, M., Mathews, R.P., Singh, B.D., Singh, H., Singh, V.P., Dutta, S., 2017a. Paleoenvironment of Eocene lignite bearing succession from Bikaner-Nagaur Basin, western India: Organic petrography, palynology, palynofacies and geochemistry. *Int. J. Coal Geol.*, 181, 87-102.
- Singh, A., Thakur, O.P., Singh, B.D., 2012a. Petrographic and depositional characteristics of Tadkeshwar lignite deposits (Cambay Basin), Gujarat. *J. Geol. Soc., India* 80, 329-340.
- Singh, H., 2020. Palaeoenvironmental and taphonomic biases in palynological assemblages preserved in amber versus sediments from the Umarsar Lignite, Kutch Basin, Gujarat, India. *Hist. Bio.*, (doi: 10.1080/08912963.2020.1791105).
- Singh, H., Judd, W.S., Samant, B., Agnihotri, P., Grimaldi, D.A., Manchester, S.R., 2021. Flowers of Apocynaceae in amber from the early Eocene of India. *Am. J. Bot.*, 108(5), 1-10.
- Singh, H., Prasad, M., Kumar, K., Singh, S.K., 2015. Early Eocene macroflora and associated palynofossils from the Cambay Shale Formation, western India: phytogeographic and palaeoclimatic implications. *Palaeoworld*, 24, 293-323.
- Singh, H., Shukla, A., Mehrotra, R.C., 2016. A Fossil Coconut Fruit from the Early Eocene of Gujarat. *J. Geol. Soc. India*, 87(3), 268-270.
- Singh, P.K., Singh, M.P., Singh, A.K., 2010. Petro-chemical characterization and evolution of Vastan lignite, Gujarat, India. *Int. J. Coal Geol.*, 82, 1-16.

- Singh, P.K., Singh, M.P., Singh, A.K., Naik, A.S., Singh, V.K., Singh, V.K., Rajak, P.K., 2012b. Petrological and geochemical investigations of Rajpardi lignite deposit, Gujarat, India. *Ener. Explor. Exploit.*, 30(1), 131-152
- Singh, V.K., Rajak, P.K., Singh, P.K., 2019. Revisiting the paleomires of western India: An insight into the early Paleogene lignite Corridor. *J. Asian Ear. Sci.*, 171, 363-375.
- Singh, V.P., Singh, B.D., Mathews, R.P., Singh, A., Mendhe, V.A., Singh, P.K., Mishra, S., Dutta, S., Shivanna, M., Singh, M.P., 2017c. Investigation on the lignite deposits of Surkha mine (Saurashtra Basin, Gujarat), western India: Their depositional history and hydrocarbon generation potential. *Int. J. Coal Geol.*, 183, 78-99.
- Singh, V.P., Singh, B.D., Singh, A., Singh, M.P., Mathews, R.P., Dutta, S., Mendhe, V.A., Mahesh, S., Mishra, S., 2017b. Depositional palaeoenvironment and economic potential of Khadsaliya lignite deposits (Saurashtra Basin), western India: Based on petrographic, palynofacies and geochemical characteristics. *Int. J. Coal Geol.*, 171, 223-242.
- Sinitshenkova, N.N., 2002. Ecological history of the aquatic insects. In: Rasnitsyn, A.P., Quicke, D.L.J., (Eds.), *History of Insects*. Dordrecht etc. Kluwer Academic Publishers, pp. 388-417
- Sluijs, A., Brinkhuis, H., Schouten, S., Bohaty, S.M., John, C.M., Zachos, J.C., Sinninghe Damste, J. S., Crouch, E.M., Dickens, G.R., 2007. Environmental precursors to light carbon input at the Paleocene/Eocene boundary. *Nature*, 450, 1218-1221.
- Smith, T., Rana, R., Missiaen, P., Rose, K.D., Sahni, A., Singh, H., Singh, L., 2007. High Bat (Chiroptera) diversity in the Early Eocene of India. *Naturwissenschaften*, 94, 1003-1009.
- Smith, T., Kumar, K., Rana, R.S., Folle, A., Sole, F., Noiret, C., Steeman, T., Sahni, A., Rose, K.D., 2016. New early Eocene vertebrate assemblage from western India reveals a mixed fauna of European and Gondwana affinities. *Geosci. Front.*, 7(6), 969-1001.
- Snowdon, L.R., 1995. Rock-Eval T_{max} suppression: Documentation and amelioration. *AAPG Bull.*, 79, 1337-1348.
- Stebner, F., Szadziwski, R., Rühr, P.T., Singh, H., Hammel, J., Kvifte, G.M., Rust, J., 2016. A fossil biting midge (Diptera: Ceratopogonidae) from early Eocene amber with a complex pheromone evaporator. *Sci. Rep.*, 6 (1), 1-8.
- Stebner, F., Szadziwski, R., Singh, H., Gunekel, S., Rust, J., 2017. Biting midge (Diptera: Ceratopogonidae) from Cambay amber indicate that the Eocene fauna of the Indian Subcontinent was not isolated. *PLoS ONE*, 12 (1), 1-24.
- Stock, A.T., Littke, R., Lücke, A., Zieger, L., Thielemann, T., 2016. Miocene depositional environment and climate in western Europe: the lignite deposits of the Lower Rhine Basin, Germany. *Int. J. Coal Geol.*, 157, 2-18.
- Stout, S.A., 1992. Aliphatic and aromatic triterpenoid hydrocarbons in a Tertiary angiospermous lignite. *Org. Geochem.*, 18(1), 51-66.
- Suárez-Ruiz, I., Flores, D., Mendonça Filho, J.G., Hackley, P.C., 2012. Review and update of the applications of organic petrology: Part 1, Geological applications. *Int. J. Coal Geol.*, 22, 54-112.

- Sudhakar, R., Basu, D.N., 1973. A reappraisal of the stratigraphy of southern Cambay Basin. *ONGC Bull.*, 10, 55-76,
- Svensen, H., Planke, S., Malthe-Sørensen, A., Jamtveit, B., Myklebust, R., Eidem, T.R., Rey, S.S., 2004. Release of methane from a volcanic basin as a mechanism for initial Eocene global warming. *Nature*, 429, 542-545.
- Sykes, R., Snowdon, L., 2002. Guidelines for assessing the petroleum potential of coaly source rocks using Rock-Eval. *Org. Geochem.*, 33(12), 1441-1455
- Sýkorová, I., Pickel, W., Christanis, K., Wolf, M., Taylor, G.H., Flores, D., 2005. Classification of huminite— ICCP System 1994. *Int. J. Coal Geol.*, 62, 85-106.
- Taylor, G.H., Teichmüller, M., Davis, A., Diessel, C.F.K., Littke, R., Robert, P., 1998. *Organic Petrology*. Gebrüder Borntraeger, Berlin.
- Tissot, B.P., Welte, D.H., 1984. *Petroleum Formation and Occurrence*. 2nd Edition, Springer: Berlin-Heidelberg-New York.
- Traverse, A., 1988. *Palaeopalynology*. Unwinhyman, Boston.
- Tripathi, S.K.M., 1994. New angiosperm pollen from subsurface Early Palaeogene sediments of Barmer District, Rajasthan, India. *Palaeobotanist*, 42(1), 61-65.
- Tripathi, S.K.M., Srivastava, D., 2012. Palynology and Palynofacies of the Early Palaeogene lignite bearing succession of Vastan, Cambay Basin, Western India. *Acta Palaeobot.* 52(1), 157-175.
- Tyson, R.V., 1993. Palynofacies analysis. In: Jenkins, D.G. (Ed.), *Applied Micropaleontology*. Kluwer Academic Publishers, Dordrecht, The Netherlands, pp. 153-191.
- Tyson, R.V., 1995. *Sedimentary Organic Matter; Organic Facies and Palynofacies*. Chapman & Hall, London.
- Venkatachala, B.S., Kar, R.K., 1969. Palynology of the Tertiary sediments of Kutch-1. Spores and pollen bore hole no. 14. *Palaeobotanist*, 17(2), 157-178.
- Wang, H., Matzke-karasz, R., Horne, D. J., Zhao, X., Cao, M., Zhang, H., Wang, B., Wang, H., Wang, B., 2020. Exceptional preservation of reproductive organs and giant sperm in Cretaceous ostracods. *Proc. R. Soc. B.*, 287, 1–8.
- Wüst, R.A.J., Hawke, M.I., Bustin, R.M., 2001. Comparing maceral ratios from tropical peat lands with assumptions from coal studies: do classic coal petrographic interpretation methods have to be discarded? *Int. J. Coal Geol.*, 48, 115-132.
- Yang, S., Horsfield, B., 2020. Critical review of the uncertainty of Tmax in revealing the thermal maturity of organic matter in sedimentary rocks *Int. J Coal Geol.*, 225, 103500.
- Zachos, J.C., Dickens, G.R., Zeebe, R.E., 2008. An early Cenozoic perspective on greenhouse warming and carbon-cycle dynamics. *Nature*, 451, 279-283.
- Zhang, S., Tang, S., Tang, D., Pan, Z., Yang, F., 2010. The characteristics of coal reservoir pores and coal facies in Liulin district, Hedong coal field of China. *Int. J. Coal Geol.*, 81, 117-127.

- Zhang, Y.G., 1979. The origin of petroleum and microbes. *Petro. Geol. Exp.*, 1, 53-63.
- Zheng, Y., Zhou, W., Meyers, P.A., Xie, S., 2007. Lipid biomarkers in the Zoigê–Hongyuan peat deposit: indicators of Holocene climate changes in West China. *Org. Geochem.*, 38, 1927-1940.
- Zhou, W.J., Xie, S.C., Meyers, P.A., Zheng, Y.H., 2005. Reconstruction of late-glacial and Holocene climate evolution in southern China from geolipids and pollen in the Dingnan peat sequence. *Org. Geochem.*, 36, 1272-1284.
- Životić, D., Jovančićević, B., Schwarzbauer, J., Cvetković, O., Gržetić, I., Ercegovac, M., Stojanović, K., Šajnović, A., 2010. The petrographical and organic geochemical composition of coal from the East field, Bogovina Basin (Serbia). *Int. J. Coal Geol.*, 81, 227-241.
- Zubov, I.P., Naugolny, I.K., Zapivalov, N.P., Chandra, D., 1966. Problem of correlation and distribution of hydrocarbon bearing horizons in the Eocene of Camaby Basin. *Bull. ONGC*, 3(2), 9-13.

Table: 1 Maceral contents (vol.%), mineral matter content (vol.%), ulminite reflectance (R_r %) and petrographic indices (GI, TPI, GWI, VI) of the studied Valia lignites.

Sample No.	V-1	V-2	V-3	V-4	V-5	V-6	V-7	V-8	V-9	V-10	V-11	V-12	V-13	Avg.
Huminite(H)	63	76	76	71	63	70	64	68	65	73	70	60	52	67
Telohuminite	26	49	44	28	31	23	22	30	28	29	19	21	2	27
Textinite	1	1	1	1	2	2	1	3	2	3	2	1	1	
Ulminite	25	47	43	27	30	22	21	27	25	27	17	20	2	
Detrohuminite	35	25	30	42	24	45	35	37	34	42	48	36	49	37
Attrinite	12	4	2	4	2	9	5	7	4	5	5	8	1	
Densinite	23	20	28	38	22	37	30	30	30	36	43	28	48	
Gelohuminite	2	2	2	1	8	2	7	1	3	2	3	3	1	3
Corpohuminite	2	2	2	1	8	2	7	1	3	2	3	3	1	
Liptinite (L)	21	15	16	24	18	21	19	10	20	14	18	15	20	17
Sporinite	3	2	1	2	3	1	2	2	4	1	0	2	0	
Cutinite	6	3	1	2	6	4	5	0	4	2	0	2	0	
Suberinite	2	1	1	5	0	3	1	1	1	1	2	1	1	
Resinite	5	5	7	11	7	8	5	5	4	5	7	5	17	
Alginite	0	0	0	0	2	0	2	0	2	0	3	3	0	
Bituminite	1	0	1	1	0	0	0	0	1	1	0	0	0	
Exsudatinitite	0	0	0	0	0	0	0	0	1	0	0	0	0	
Liptodetrinite	4	4	5	3	0	5	4	2	3	4	6	2	2	
Inertinite (I)	7	3	5	1	9	5	8	10	10	8	4	4	1	6
Semifusinite	1	0	1	0	1	1	1	1	0	1	1	1	0	
Funginite	3	2	3	0	4	3	5	8	7	4	3	1	0	
Inertodetrinite	3	1	1	1	4	1	2	1	3	3	0	2	1	
Mineral Matter (M)	8	5	6	4	9	4	9	13	7	5	8	20	27	10
Other	6	4	5	2	5	3	4	9	5	3	6	12	25	

	Pyrite	2	1	1	2	4	1	5	4	2	2	2	8	2	
Fluorescing H		19	23	25	26	22	18	22	17	22	18	26	17	14	21
Non-fluorescing (H)		45	52	50	45	41	53	42	51	42	55	44	43	38	46
Total Fluorescing (H+L)		40	39	40	49	41	38	42	27	41	32	44	32	34	38
Non-fluorescing (H+I+M)		60	61	60	51	59	62	58	73	59	68	56	68	66	62
H (mmf)		69	80	79	75	69	74	70	78	69	77	76	75	71	74
L (mmf)		23	17	16	24	21	21	21	11	21	15	20	20	28	20
I (mmf)		8	3	5	1	10	5	9	11	10	8	4	5	1	6
R _r mean %		0.29	0.3	0.27	0.26	0.28	0.29	0.29	0.28	0.3	0.28	0.28	0.29	0.27	0.28
GI		2.52	7.74	10.36	12.37	4.52	3.79	4.04	2.96	3.6	4.06	5.76	3.78	26.47	7.07
TPI		0.75	1.95	1.49	0.68	1.38	0.54	0.78	0.82	0.84	0.71	0.45	0.62	0.06	0.85
GWI		0.74	0.47	0.71	1.35	0.96	1.52	1.47	0.95	1.09	1.17	2.03	1.37	18.13	2.46
VI		0.99	1.99	1.51	1.03	1.29	0.78	0.8	0.96	0.9	0.78	0.51	0.74	0.39	0.97
GI (Gelification Index) = Ulminite+Densinite+Corpohuminite+Gelinite / Textinite+Attrinite+Inertinite (Kalaitzidis et al., 2004)															
TPI (Tissue Preservation Index) = Textinite+Ulminite+Corpohuminite+Fusinite / Attrinite+Densinite+Gelinite+Inertodetrinite (Kalaitzidis et al., 2004)															
GWI (Ground Water Index) = Densinite+Corpohuminite+Gelinite+(Ash/2) / Textinite+Ulminite+Attrinite (Kalaitzidis et al., 2004; Stock et al., 2016)															
VI (Vegetation Index) =Textinite+Ulminite+Sporinite+Cutinite+Suberinite+Resinite+Fusinite+Semifusinite / Attrinite+Densinite+Alginite+Bituminite+ Liptodetrinite+Inertodetrinite (Kalaitzidis et al., 2004)															

Table 2: Result of palynofacies analysis of the studied Valia samples.

S. No	Phytoclasts					Total (%)	AOM		Total (%)	Palynomorphs (%)	PF Type
	O (%)	N-O					AOM (%)	R (%)			
		B (%)	NB (%)	C (%)	F (%)						
VA-51	10	0	19	0	0	29	71	0	71	0	III
VA-50	7	0	20	0	0	27	72	0	72	0	III
VA-49	5	0	20	1	2	28	70	1	71	1	III
VA-48	0	2	50	16	2	70	31	0	31	0	I
VA-47	0	1	71	13	2	87	10	0	10	4	I
VA-46	0	1	49	9	1	60	40	0	40	0	I
VA-45	0	0	50	3	0	53	47	0	47	0	II
VA-44	0	0	64	10	0	74	27	0	27	0	I
VA-43	0	0	39	4	0	43	57	0	57	1	II
VA-42	0	0	44	6	0	50	51	0	51	0	II
VA-41	0	0	45	1	0	46	52	2	54	0	II
VA-40	0	0	37	15	0	52	48	0	48	0	II
VA-39	0	0	41	8	0	49	52	0	52	0	II
VA-38	0	0	82	5	0	87	12	0	12	0	I
VA-37	0	0	69	8	0	77	23	0	23	0	I
VA-36	0	0	70	5	2	77	23	0	23	1	I
VA-35	0	0	36	10	0	46	54	0	54	0	II
VA-34	4	0	58	22	0	84	17	0	17	0	I
VA-33	2	1	51	22	0	76	25	0	25	0	I
VA-32	2	0	51	24	1	78	22	0	22	0	I
VA-31	0	1	55	23	1	80	20	0	20	1	I
VA-30	1	0	50	35	1	87	13	0	13	1	I
VA-29	3	1	57	18	1	80	19	0	19	2	I
VA-28	1	0	20	58	1	80	20	0	20	0	I
VA-27	2	0	65	15	2	84	15	0	15	0	I
VA-26	1	0	63	15	0	79	20	0	20	1	I
VA-25	0	0	63	17	0	80	21	0	21	0	I
VA-24	7	1	62	3	1	74	26	0	26	0	I
VA-23	4	2	67	2	1	76	24	0	24	1	I
VA-22	2	1	68	3	1	75	25	1	26	0	I
VA-21	2	0	72	2	0	76	23	0	23	0	I
VA-20	0	0	37	3	5	45	55	0	55	0	II
VA-19	0	0	45	3	1	49	52	0	52	0	II

VA-18	0	0	52	3	0	55	45	0	45	0	II
VA-17	0	0	43	2	0	45	55	0	55	0	II
VA-16	0	0	46	0	0	46	53	0	53	0	II
VA-15	0	0	49	4	0	53	46	0	46	0	II
VA-14	0	0	52	2	1	55	45	0	45	0	II
VA-13	0	0	40	2	0	42	58	0	58	0	II
VA-12	0	0	46	0	0	46	54	0	54	0	II
VA-11	0	0	42	4	0	46	53	0	53	0	II
VA-10	0	0	41	9	0	50	50	0	50	0	II
VA-9	0	0	42	10	1	53	48	0	48	0	II
VA-8	0	0	38	19	0	57	39	3	42	0	II
VA-7	0	0	40	9	2	51	48	0	48	0	II
VA-6	0	2	42	7	1	52	46	2	48	0	II
VA-5	0	0	54	11	1	66	34	0	34	0	I
VA-4	0	0	38	29	0	67	32	0	32	0	I
VA-3	0	0	40	30	0	70	30	0	30	0	I
VA-2	0	0	22	26	1	49	52	0	52	0	I
VA-1	0	0	62	0	4	66	33	0	33	2	I
Min.	0	0	19	0	0	27	10	0	10	0	
Max	10	2	82	58	5	87	72	3	72	4	
Average	1	0	48	11	1	61	38	0	39	0	

O= Opaque; N-O= Non-opaque; C= Cuticle; B= Biostructured; NB= Non-biostructured; F= Fungal; AOM= Amorphous Organic Matter; R= Resin; PF= Palynofacies.

Table 3: Arthropods from Valia Amber.

Class	Order	Tribe/Family/Genus	Habitat suitability	Composition (%)
Insecta	Diptera	Chironomidae	Tropical, sub-tropical lowlands, Temperate	32
		Cecidomyiidae	Wet region	13
		Mycetophilidae	Wet and moist region	10
	Hymenoptera	<i>Myrmecia</i> ; Myrmicinae	Humid region	19
Arachnida	Araneae	Sicariidae, Actinopodidae	Moisture-rich areas	25
	Pseudoscorpionida	Pseudoscorpiones	Warmer climate, Temperate regions	1

Table 4: Values of *n*-alkane and various calculated indices/ratios from the studied Valia samples.

Lithology	Sample	Pr/Ph	Pr/ <i>n</i> -C ₁₇	Ph/ <i>n</i> -C ₁₈	P _{wax}	P _{aq}	CPI	TAR	ACL	□C ₂₂₋ / □C ₂₃₊
Carb. Shale	V-30	1.61	0.75	0.44	0.69	0.5	2.33	2.56	22.32	0.50
	V-27	2.01	1.13	0.51	0.70	0.47	2.38	2.07	23.25	0.65
Shale	V-32	0.60	0.37	0.58	0.66	0.51	3.04	1.23	21.63	1.08
	V-12	0.89	0.47	0.45	0.27	0.85	1.65	0.05	15.71	9.45
Lignite	V-41	1.14	3.10	2.64	0.40	0.71	2.63	0.10	21.16	7.10
	V-38	0.43	0.31	0.31	0.58	0.64	5.94	0.25	21.81	9.93
	V-29	0.91	0.54	0.44	0.22	0.88	1.60	0.07	16.45	6.10
	V-8	0.44	0.32	0.31	0.59	0.64	5.72	0.26	22.18	9.25
	V-5	0.90	0.52	0.43	0.41	0.71	2.79	0.10	20.78	7.87
Min.		0.43	0.31	0.31	0.22	0.47	1.60	0.05	15.71	0.50
Max.		2.01	3.10	2.64	0.70	0.88	5.94	2.56	23.25	9.93
Avg.		0.99	0.83	0.68	0.5	0.66	3.12	0.74	20.59	5.77

Pr: Pristane, Ph: Phytane, P_{aq}: Proxy aqueous, P_{wax}: Proxy wax, CPI: Carbon Preference Index, TAR: Terrigenous/Aquatic Ratio, ACL: Aliphatic chain length

$$P_{wax} = (C_{23} + C_{25}) / (C_{23} + C_{25} + C_{29} + C_{31})$$

Zheng et al. (2007).

$$P_{aq} = (C_{27} + C_{29} + C_{31}) / (C_{23} + C_{25} + C_{27} + C_{29} + C_{31})$$

Ficken et al. (2000).

$$CPI = 2(C_{23} + C_{25} + C_{27} + C_{29}) / [C_{22} + 2(C_{24} + C_{26} + C_{28}) + C_{30}]$$

Peters et al. (2005).

$$TAR = (C_{27} + C_{29} + C_{31}) / (C_{15} + C_{17} + C_{19})$$

Bourbonniere and Meyers (1996).

$$ACL = [(25C_{25} + 27C_{27} + 29C_{29} + 31C_{31} + 33C_{33}) / (C_{25} + C_{27} + C_{29} + C_{31} + C_{33})]$$

Eglinton and Hamilton, (1967).

Table 5: Biomarker compounds identified in the studied Valia lignite and shale samples.

Sl. no	Compound name	Mol. mass	id
<i>Bicyclic sesquiterpanes</i>			
1	4 β (H)-eudesmane	208	Sq1
2	8 β (H)-drimane	208	Sq3
3	8 β (H)-homodrimane	222	Sq4
<i>Diterpenoids</i>			
4	<i>ent</i> -Kaurane	274	d1
5	Isopimarane	276	d2
6	19-norisopimarane	262	d3
<i>Tetracyclic triterpenoids</i>			
7	Isomer of De-A-olean-13(18)-ene?	328	dt1
8	Isomer of De-A-olean-13(18)-ene	328	dt2
9	Unidentified De-A-triterpenoid	328	dt3
10	Compound 'A' (Stout, 1992)	326	dt4
11	De-A-olean-12-ene	328	dt5
12	De-A-Lupane	330	dt6
13	Unidentified De-A-triterpenoid	328	dt7
14	De-A-Ursane?	330	dt8
<i>Secohopanes</i>			
15	17,21-secohopane (C25)	344	s1
16	17,21-secohopane (C26)	358	s2
<i>Pentacyclic triterpenoids</i>			
17	22,29,30-Trisnorneohop-13(18)-ene	368	1
18	17 β (H)-22,29,30-Trisnorhopane	370	2
19	30-Norneohop-13(18)-ene	396	3
20	Neohop-13(18)-ene	410	4
21	Olean-12-ene	410	5
22	$\beta\alpha$ -30-Norhopane	398	6
23	Neohop-13(18)-ene	410	7
24	$\beta\beta$ -30-Norhopane	398	8
25	$\alpha\beta$ -Homohopane (22 S)	426	9
26	$\alpha\beta$ -Homohopane (22 R)	426	10
27	$\beta\beta$ -hopane	412	11
28	$\beta\beta$ -Homohopane	426	12
<i>Aromatic triterpenoids</i>			
29	24,25-Dinoroleana-1,3,5(10),12-tetraene	376	a1
30	24,25-Dinorursa-1,3,5(10),12-tetraene	376	a2
31	Dinoroleana-1,3,5(10),12-triene	378	a3
32	Diaromatic pentacyclic triterpane	374	a4

Table 6. Results of proximate and ultimate analyses of the studied Valia lignites.

S. No.	As received basis		Air-dry basis (db) wt. %		Dry ash-free basis (daf) (wt. %)						Atomic ratio		Fuel Ratio (wt. %)
	GCV (Cal/g)	M (wt. %)	Ash	S	VM	FC	C	H	N	O	O/C	H/C	
V-1	4531	32.54	4.58	2.24	53.82	46.18	79.07	4.24	0.80	18.34	0.19	0.71	0.86
V-2	4816	28.97	4.6	1.93	51.08	48.92	78.97	3.20	1.97	19.34	0.20	0.53	0.96
V-3	4637	30.04	5.48	2.05	53.09	46.91	78.32	2.94	1.73	22.99	0.25	0.52	0.88
V-4	4689	28.72	6.58	1.64	62.44	37.56	62.01	3.02	1.86	29.54	0.36	0.58	0.60
V-5	3824	41.7	3.82	1.36	51.63	48.37	73.11	2.85	2.90	25.93	0.30	0.53	0.94
V-6	3279	33.04	19.79	1.52	58.19	41.81	68.67	3.86	1.65	21.01	0.23	0.67	0.72
V-7	5123	24.11	5.29	1.43	51.73	48.27	67.71	2.88	2.07	24.67	0.27	0.51	0.93
V-8	3965	35.97	8.19	1.27	56.75	43.25	65.98	3.30	1.87	25.29	0.29	0.60	0.76
V-9	5216	23.38	4.17	1.78	56.65	43.35	58.04	2.68	1.73	34.34	0.44	0.55	0.77
V-10	5042	25.83	4.09	1.25	55.99	44.01	60.08	3.61	1.44	32.46	0.41	0.72	0.79
V-11	4061	35.13	6.71	0.69	69.27	30.73	73.26	2.96	1.70	20.26	0.21	0.48	0.44
V-12	4272	22.62	17.79	0.87	65.55	34.45	63.74	5.03	1.26	28.09	0.33	0.94	0.53
V-13	4619	15.76	19.02	1.72	75.68	24.32	60.68	6.56	1.49	28.14	0.35	1.29	0.32
Min.	3279	15.76	3.82	0.69	51.08	24.32	58.04	2.68	0.80	18.34	0.19	0.48	0.32
Max.	5216	41.70	19.79	2.24	75.68	48.92	79.07	6.56	2.90	34.34	0.44	1.29	0.96
Avg.	4467	29.06	8.47	1.52	58.61	41.39	68.43	3.63	1.73	25.41	0.30	0.66	0.73

M= Moisture; VM= Volatile matter; FC= Fixed Carbon; GCV= Gross Calorific Value, Min= Minimum, Max.=Maximum, Avg.= Average.

Table 7. Results of Rock-Eval Pyrolysis and calculated parameters of the studied Valia samples.

Lithology	Sample	S1	S2	S3	TOC	T _{max}	HI	OI	PI	GP	S2/S3
Lignite	VA-47	14.14	372.1	16.65	53.64	396	694	31	0.04	386.2 4	22.35
	VA-43	6.71	84.93	24.92	35.9	379	236	69	0.07	91.64	3.41
	VA-35	7.89	140.3	27.78	55.6	383	252	50	0.05	148.2 2	5.05
	VA-29	2.23	72.92	26.47	38.3	417	190	69	0.03	75.15	2.75
	VA-9	1.66	74.24	28.87	49	415	152	59	0.02	75.9	2.57
	VA-3	0.83	55.87	30.93	44.9	410	124	69	0.01	56.7	1.81
	VA-1	3.81	112	30.27	49.8	410	225	61	0.03	115.8 1	3.7
Min.		0.83	55.87	16.65	35.9	379	124	31	0.01	56.7	1.81
Max.		14.14	372.1	30.93	55.6	417	694	69	0.07	386.2 4	22.35
Avg.		5.32	130.3	26.56	46.7	401	268	58	0.04	135.6 7	5.95
Shale	VA-32	0.16	7.9	1.66	2.83	437	279	59	0.02	8.06	4.76
	VA-22	0.04	0.19	1.22	0.47	433	40	260	0.17	0.23	0.16
Carb. Shale	VA-30	0.94	37.01	6.28	12.2	427	302	51	0.02	37.95	5.89
	VA-27	1.07	45.07	9.42	16.2	424	278	58	0.02	46.14	4.78
Min.		0.04	0.19	1.22	0.47	424	40	51	0.02	0.23	0.16
Max.		1.07	45.07	9.42	16.2	437	302	260	0.17	46.14	5.89
Avg.		0.55	22.54	4.65	7.93	430	225	107	0.06	23.10	3.90

S1= free hydrocarbons (mgHC/g); S2= amount of hydrocarbons (mgHC/g); S3= released carbon dioxide (mg CO₂/g); TOC= Total organic carbon (wt.%); T_{max}= temperature maximum (°C); HI (Hydrogen Index) = (S2/TOC) × 100 (mg HC/g TOC); OI (Oxygen Index) = (S3/TOC) × 100 (mg CO₂/g TOC); PI (Production Index) = S1/(S1+S2); GP (Genetic Potential) = S1+S2; S2/S3= Hydrogen richness; mg/g= Milligram/gram; wt.= Weight, Min.= Minimum, Max.= Maximum, Avg.= Average.

Table 8. Modern affinity of recovered palynomorphs along with their habitat and climatic conditions.

Families	Palynotaxa	Present- day distribution	Ecological Group
Dicksoniaceae	<i>Dictyophyllidites laevigatus</i>	Cosmopolitan	Swamps/River banks
Osmundaceae	<i>Osmundacidites Kutchensis</i>	Tropical	Cosmopolitan
Osmundaceae	<i>Todiosporites plicatus</i>	Tropical-subtropical	Sub-aquatic to swampy
Matoniaceae	<i>Dandotiaspora dilata</i>	Tropical-subtropical	Aquatic to swampy
Polypodiaceae	<i>Polypodiaceoisporites fossulatus</i>	Cosmopolitan	Grow along the moist areas
Schizaeaceae	<i>Lygodiumsporites lakiensis</i>	Tropical-subtropical	Freshwater swamp
Schizaeaceae	<i>Lygodiumsporites pachyexinus</i>	Tropical-subtropical	Climbing ferns
Arecaceae	<i>Spinizonocolpites Venkatachala</i>	Tropical-subtropical	Evergreen forest, back mangrove, Deltaic
Arecaceae	<i>Proxapertites microreticulatus</i>	Chiefly tropical	Climbers in evergreen forest, Moist temperate
Arecaceae	<i>Palmidites maximus</i>	Tropical dry forests	Coastal evergreen-rain forest
Arecaceae	<i>Kapurdipollenites gemmatus</i>	Tropical-subtropical	Evergreen forest
Arecaceae	Echinate tricolpate pollen	Tropical-subtropical	Evergreen forest
Arecaceae	<i>Neocouperipolis robustus</i>	Mostly Tropical	Coastal forest
Arecaceae	<i>Arecipites wodehousei</i>	Tropical to subtropical	Coastal evergreen-rain forest
Arecaceae	<i>Acanthotricolpites</i> spp.	Tropics to subtropics	Trees in rain forest
Arecaceae	<i>Longapertites</i> spp.	Tropics	Palms of lowland evergreen vegetation
Liliaceae	<i>Liliacidites</i> sp.	Member of coastal vegetation	Coastal vegetation - freshwater
<i>Bombacaceae</i>	<i>Lakiapollis ovatus</i>	Tropical to subtropical	Swamp and low land areas
<i>Bombacaceae</i>	<i>Dermatobrevicolporites dermatus</i>	Tropical	Swamp low land-freshwater
Rhizophoraceae	<i>Paleosantalaceaeapites minutes</i>	Tropical-subtropical	Freshwater
Caesalpiniaceae	<i>Margocolporites sahnii</i>	Tropical-subtropical	Freshwater swamp/water-edge
Ctenolophonaceae	<i>Ctenolophonidites</i> sp.	Tropical	Cosmopolitan
Miliaceae	<i>Meliapollis</i> sp. cf. <i>M. raoi</i>	Tropical-subtropical	Mangrove to freshwater
Rubiaceae	<i>Retitricolporites</i> sp.	Tropical-subtropical	Marshy herb to Cosmopolitan
Annonaceae	<i>Matanomadhiasulcites maximus</i>	Tropical	Semi-humid rain forest adjacent to coast
Ctenolophonaceae	<i>Retistephanocolpites flavatus</i>	Tropical	Freshwater swamp
Microthyriaceae	<i>Callimothallus pertusus</i>	Tropical to subtropical	Humid Forest
Microthyriaceae	<i>Phragmothyrites eocenicus</i>	Tropical to subtropical	Warm and humid forest

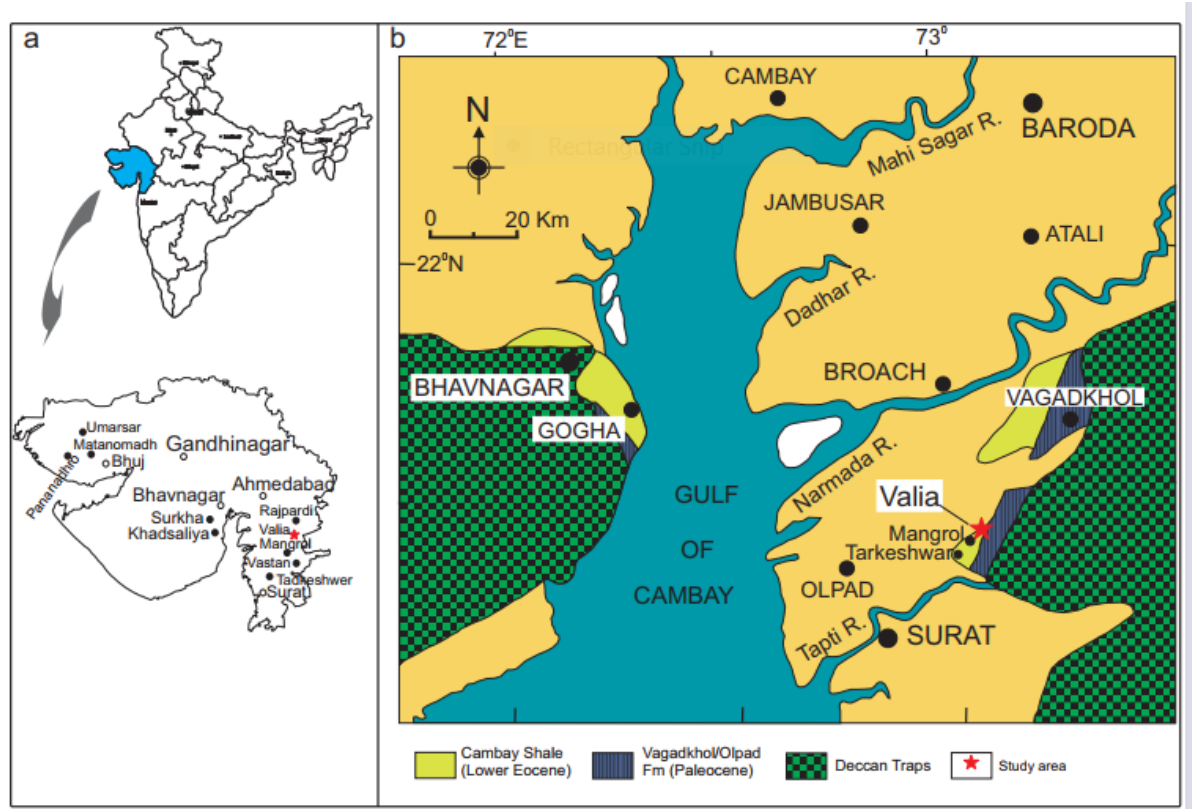


Fig. 1. Location (a) and geological map (b) of Valia lignite mine in Gujarat state, western India.

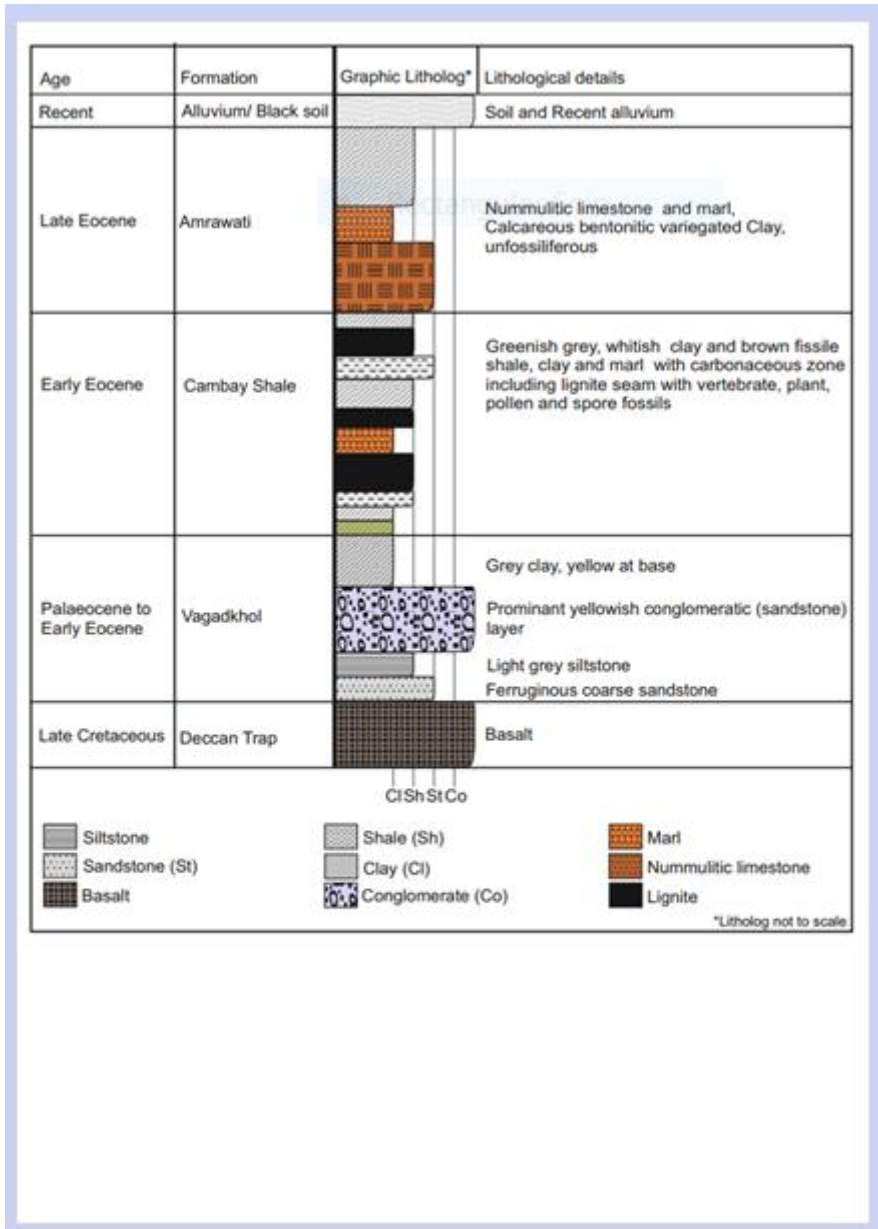


Fig. 2. A Generalized lithostratigraphic succession of Cambay Basin, western India (after Bhandari et al., 2005).

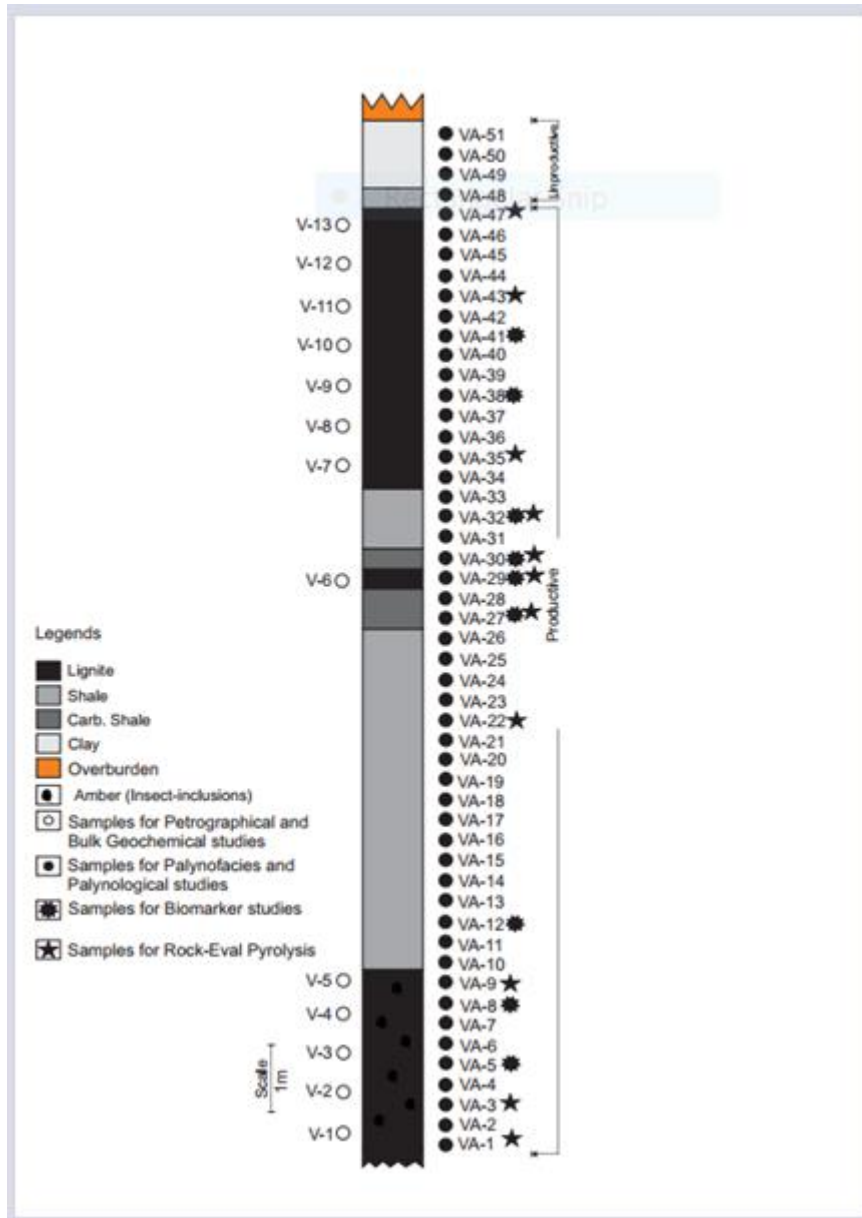


Fig. 3. Litholog of Valia lignite mine showing the lithological units and the sample positions.

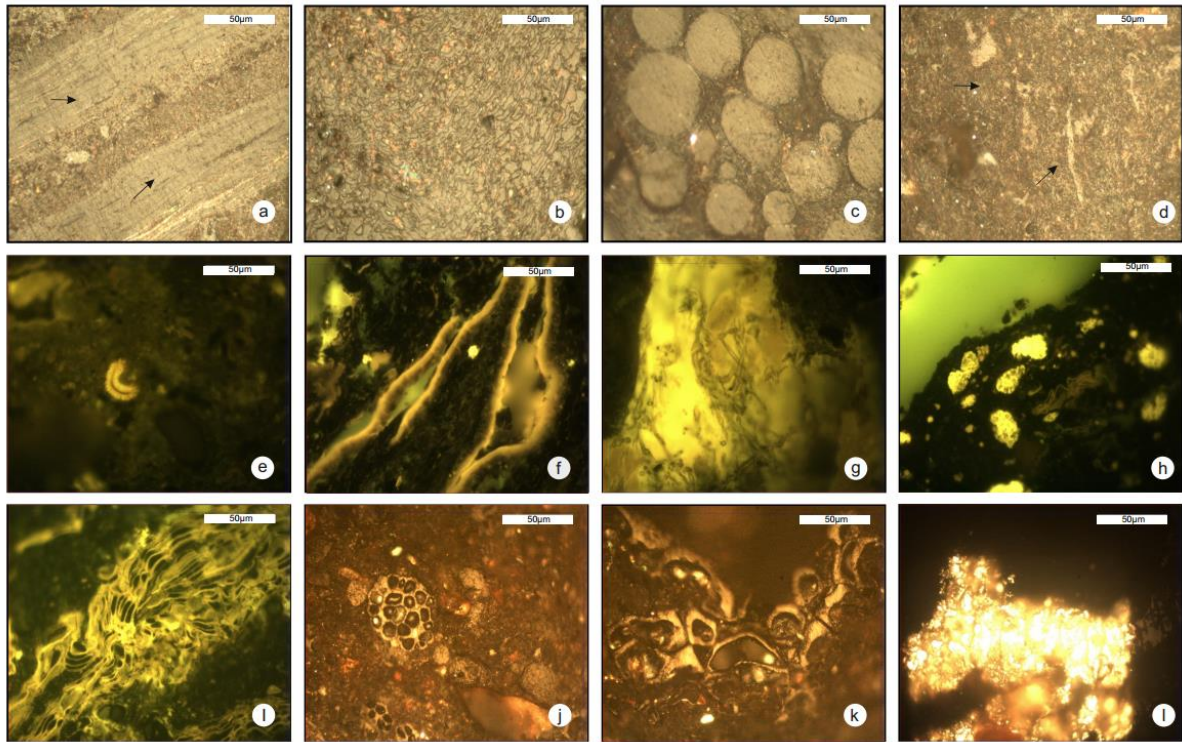


Fig. 4. Representative photomicrographs of different macerals of the studied lignite: a) ulminite (sample V-11), b) textinite (sample V-8), c) corpohuminite (sample V-7), d) densinite (sample V-6), e) sporinite (sample V-9), f) cutinite (sample V-1), g) resinite (sample V-2), h) alginite (sample V-5), i) suberinite (sample V-4), j) funginite (sample V-10), k) semifusinite (sample V-3), l) pyrite (sample V-12). Photomicrographs were taken under reflected white light (a–d and j–l) and in fluorescence mode (e–i).

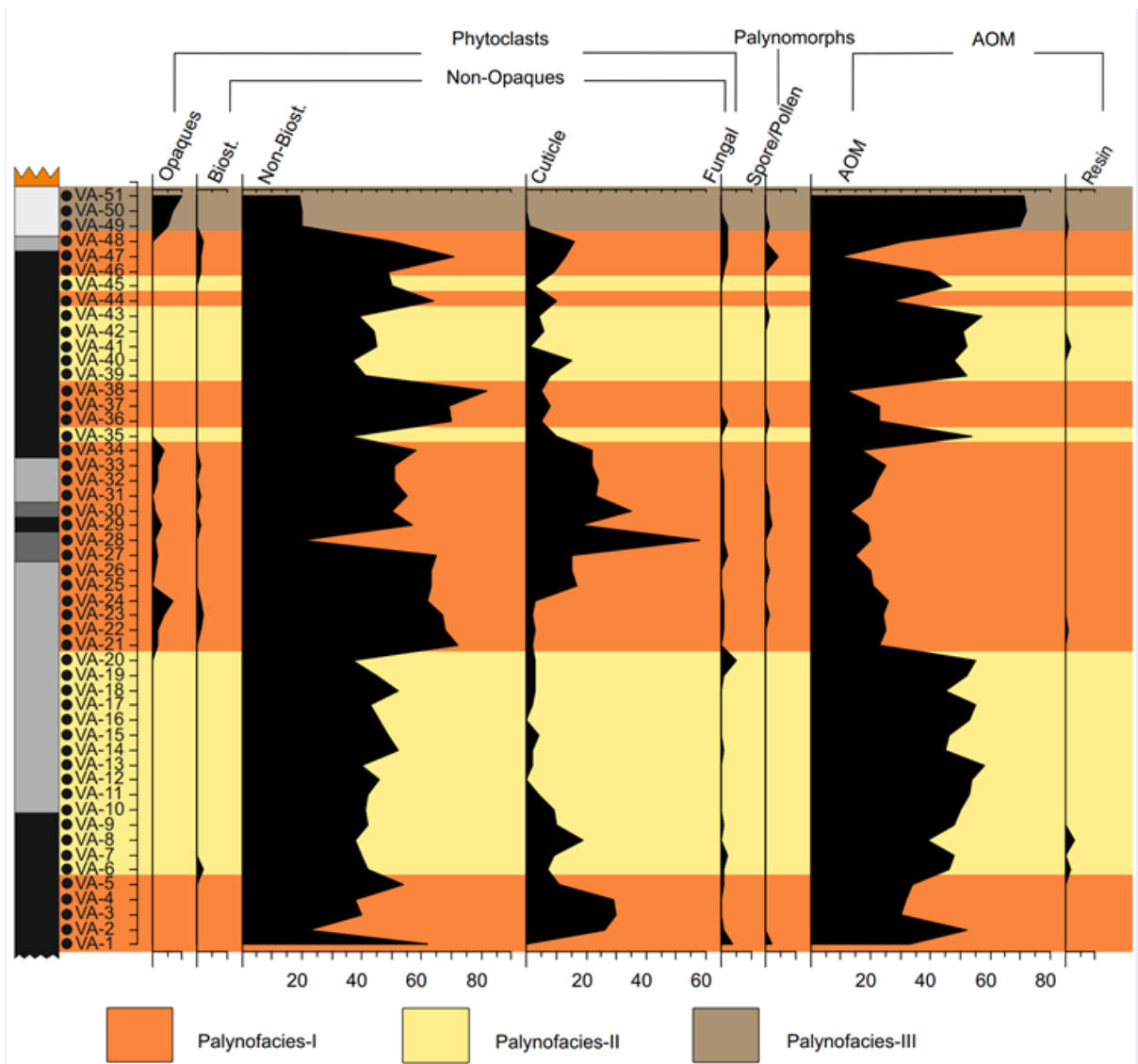


Fig. 5. Vertical distribution of different palynofacies components and the facies identified in the studied succession.

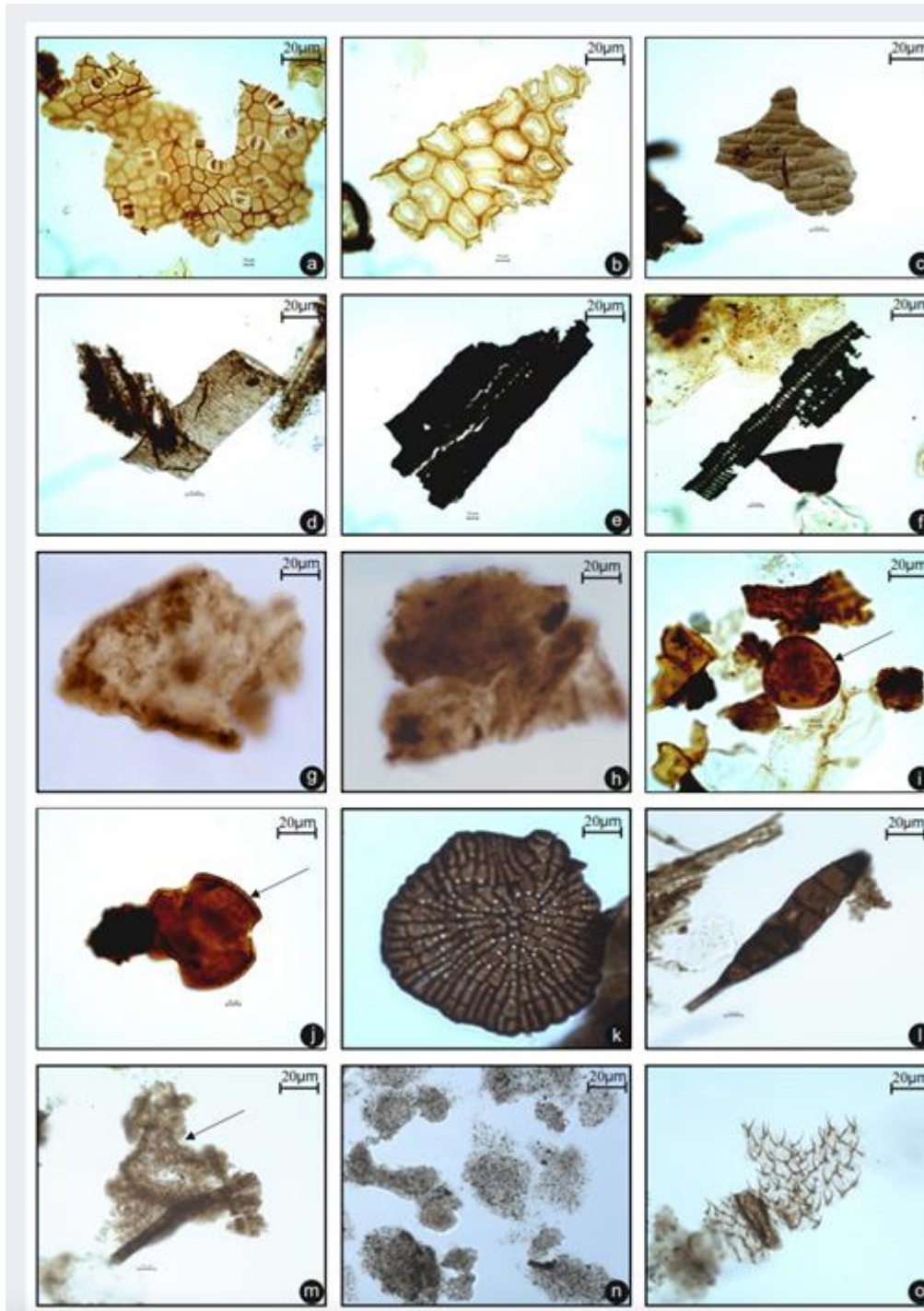


Fig. 6. Representative photomicrographs of palynofacies components: a-b) cuticle (sample VA-1), c-d) biostructured phytoclast (sample VA-1), e-f) opaque phytoclasts (sample VA-51), g-h) non-biostructured phytoclast (sample VA-3), i-j) palynomorphs (sample VA-47), k-l) fungal elements (sample VA-7), m) gelified-amorphous organic matter with fungal (sample VA-28), n) granular-amorphous organic matter (sample VA-50), o) zooclast (sample VA-51).

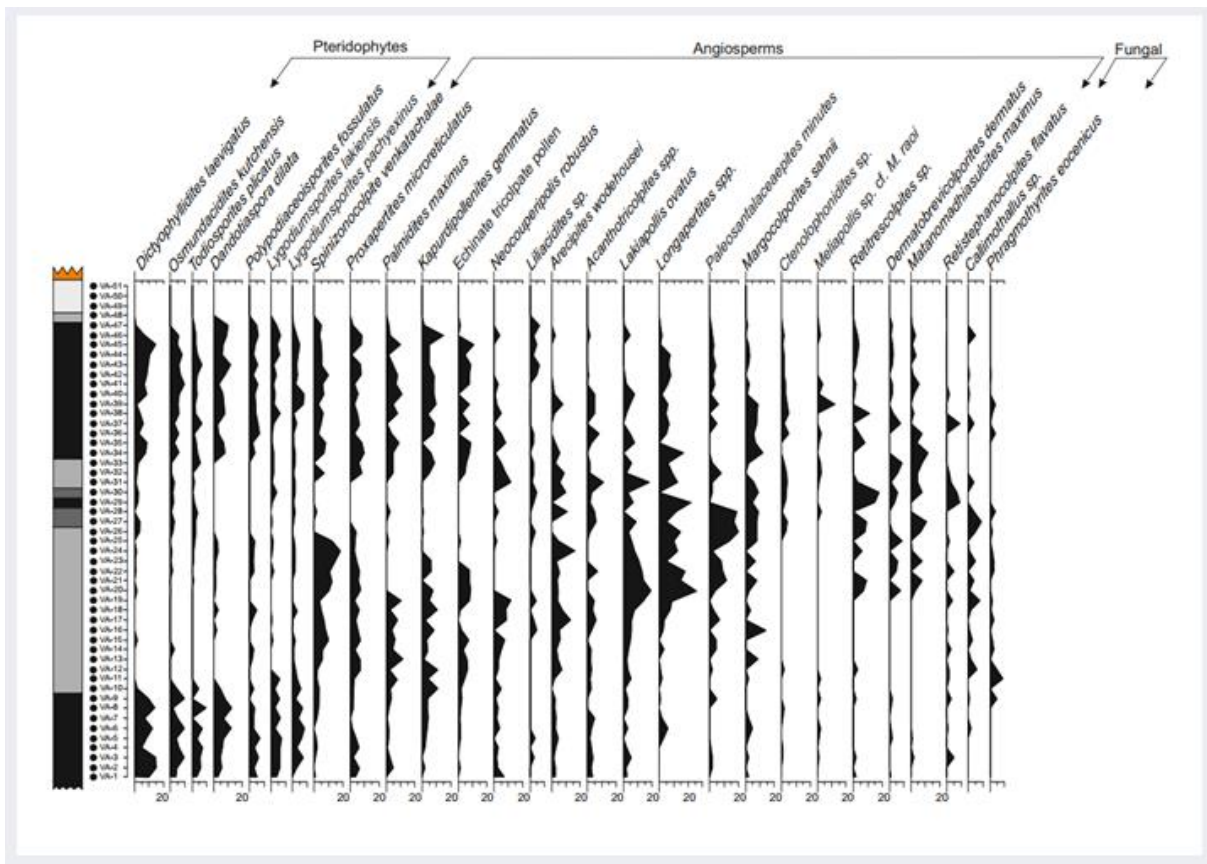


Fig. 7. Frequency distribution of different palynotaxa recovered in the Valia samples.

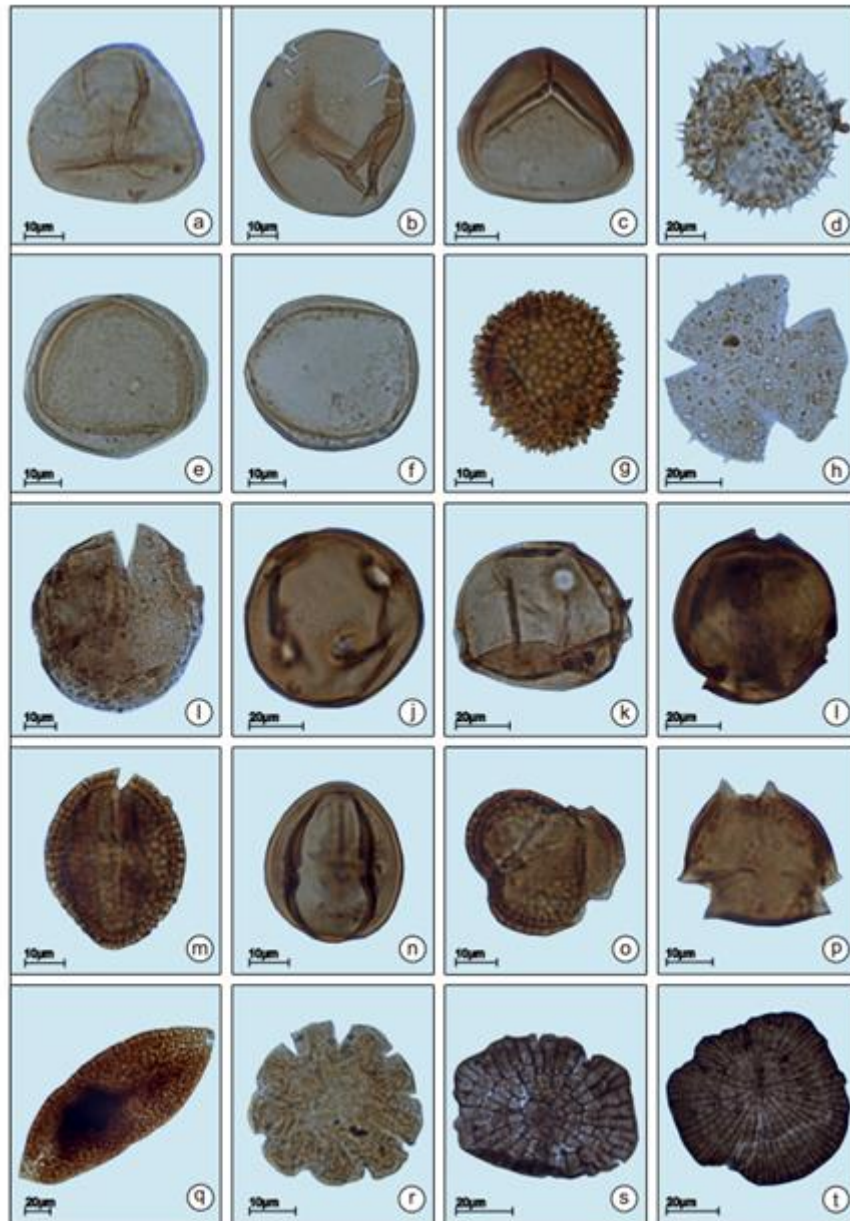


Fig. 8. Palynomorphs recovered from the studied samples: a) *Lygodiumsporites lakiensis*, Sah and Kar, 1969 (BSIP slide no. 16878); b) *Lygodiumsporites pachyexinus*, Saxena, 1978 (BSIP slide no. 16879); c) *Todiosporites kutchensis*, Sah and Kar, 1969 (BSIP slide no. 16880); d) *Spinizonocolpites venkatachala*, Saxena and Khare, 2004 (BSIP slide no. 16881); e) *Proxapertites microreticulatus*, Jain et al., 1973 (BSIP slide no. 16879); f) *Proxapertites microreticulatus*, Jain et al., 1973 (BSIP slide no. 16882); g) *Kapurdipollenites gemmatus*, Tripathi, 1994 (BSIP slide no. 16883); h) Echinete tricolpate pollen (BSIP slide no. 16884); i) *Arecipites wodehousei*, Samant and Phadtare, 1997 (BSIP slide no. 16885); j-k) *Lakiapollis ovatus*, Venkatachala and Kar, 1969 (BSIP slide no. 16886); l) *Meliapollis* sp. cf. *M. Raoi*, Sah and Kar, 1970 (BSIP slide no. 16887); m) *Retitricolporites* sp. (BSIP slide no. 16888); n) *Paleosantalaceapites minutes*, Sah and Kar, 1970 (BSIP slide no. 16879); o) *Retitricolporites* sp. (BSIP slide no. 16889); p) *Dermatobrevicolporites dermatus*, Kar, 1985 (BSIP slide no. 16890); q) *Matanomadhiasulcites maximus*, Saxena, 1979; Kar, 1985 (BSIP slide no. 16891); r) *Ctenolophonidites* sp. (BSIP slide no. 16880); s) *Callimothallus pertusus*, Dilcher, 1965 (BSIP slide no. 16881); t) *Phragmothyrites eocenicus*, Edwards, 1922 (BSIP slide no. 16880).



Fig. 9. Representative photomicrographs of amber arthropod-inclusions: a) Fungus gnat (Family Mycetophilidae), BSIP specimen no. 41976; b) Ant genus *Mymecia* (myrmicinae), BSIP specimen no. 41977; c) Recluse spider (Family Sicariidae), BSIP specimen no. 41978; d) Non-biting midge (Family Chironomidae), BSIP specimen no. 41979; e) Biting midge (Family Cecidomyiidae), BSIP specimen no. 41980; f) Mouse spider (Family Actinopodidae), BSIP specimen no. 41981; g) Pseudoscorpion (Order Pseudoscorpiones), BSIP specimen no. 41982; h) Lestremiinae (Family Cecidomyiidae), BSIP specimen no. 41983; i) Leptosynini gall midge, BSIP specimen no. 41984.

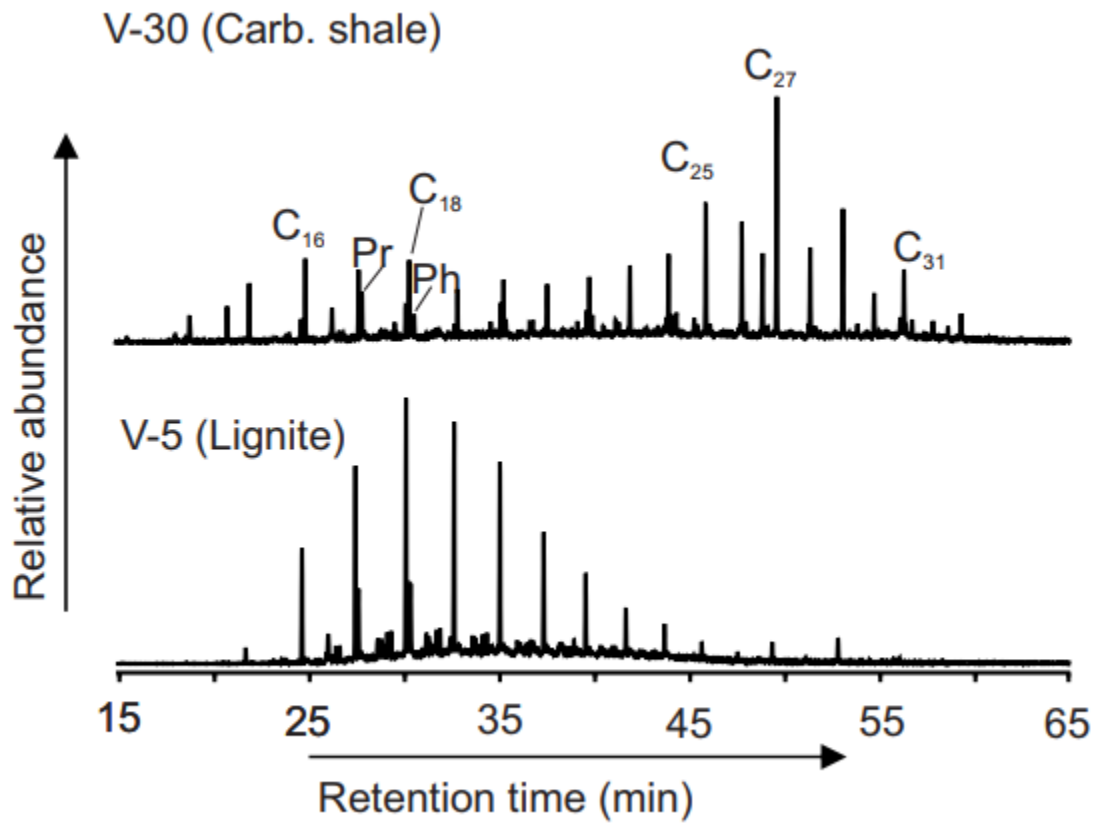


Fig. 10. *n*-alkane distribution according to SIM m/z 57 in the studied lignite samples. Numbers correspond to carbons in the *n*-alkane chain.

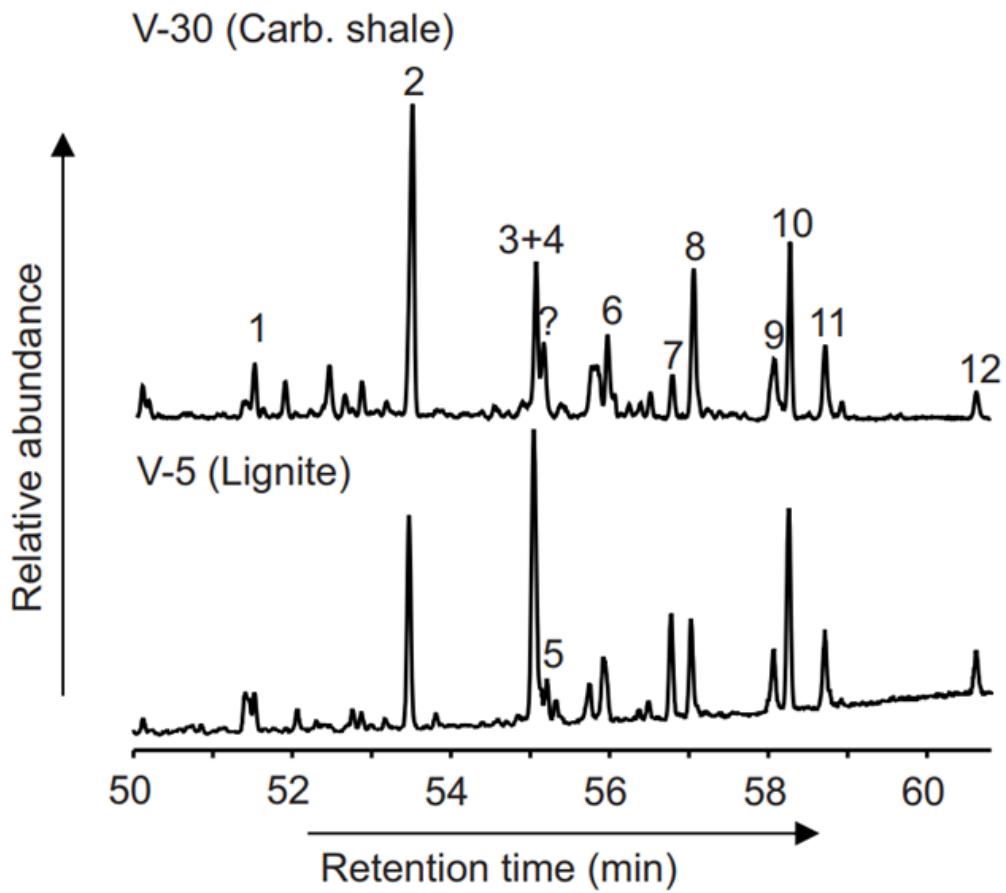


Fig. 11. Sesquiterpenoid and diterpenoid distribution m/z 123 in the studied samples. Numbers correspond to compounds referred in Table 5.

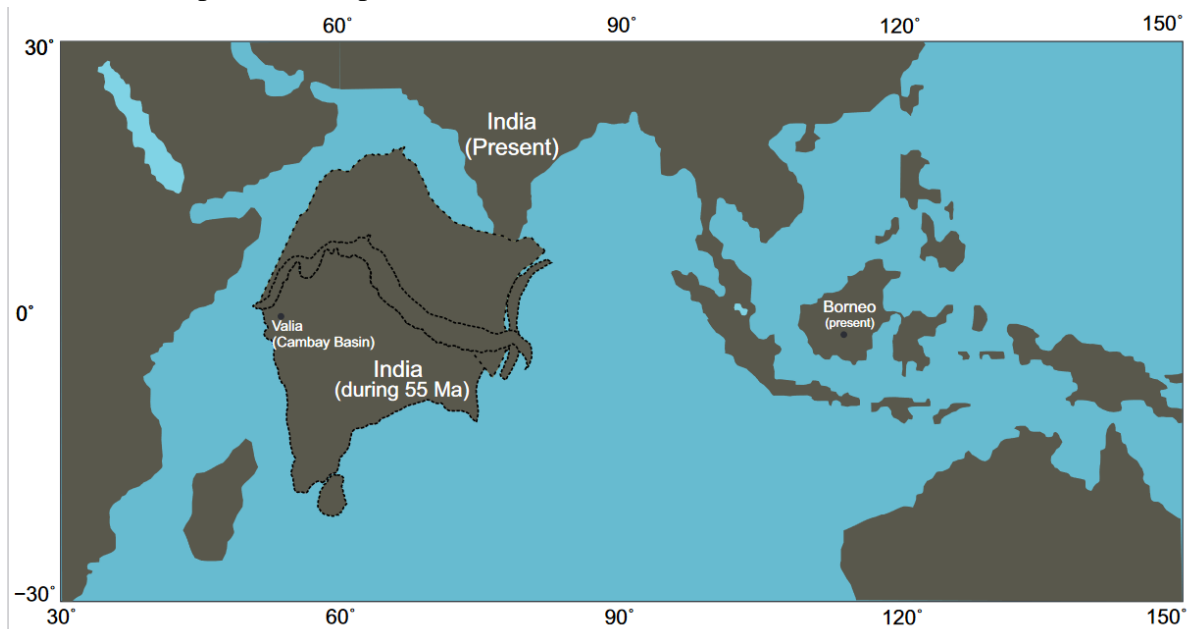


Fig. 12. A geographical map representing the palaeoposition of India (during ~ 55 Ma; <https://www.odsn.de/osdn/services/paleomap/paleomap.html>) and present position of Borneo.

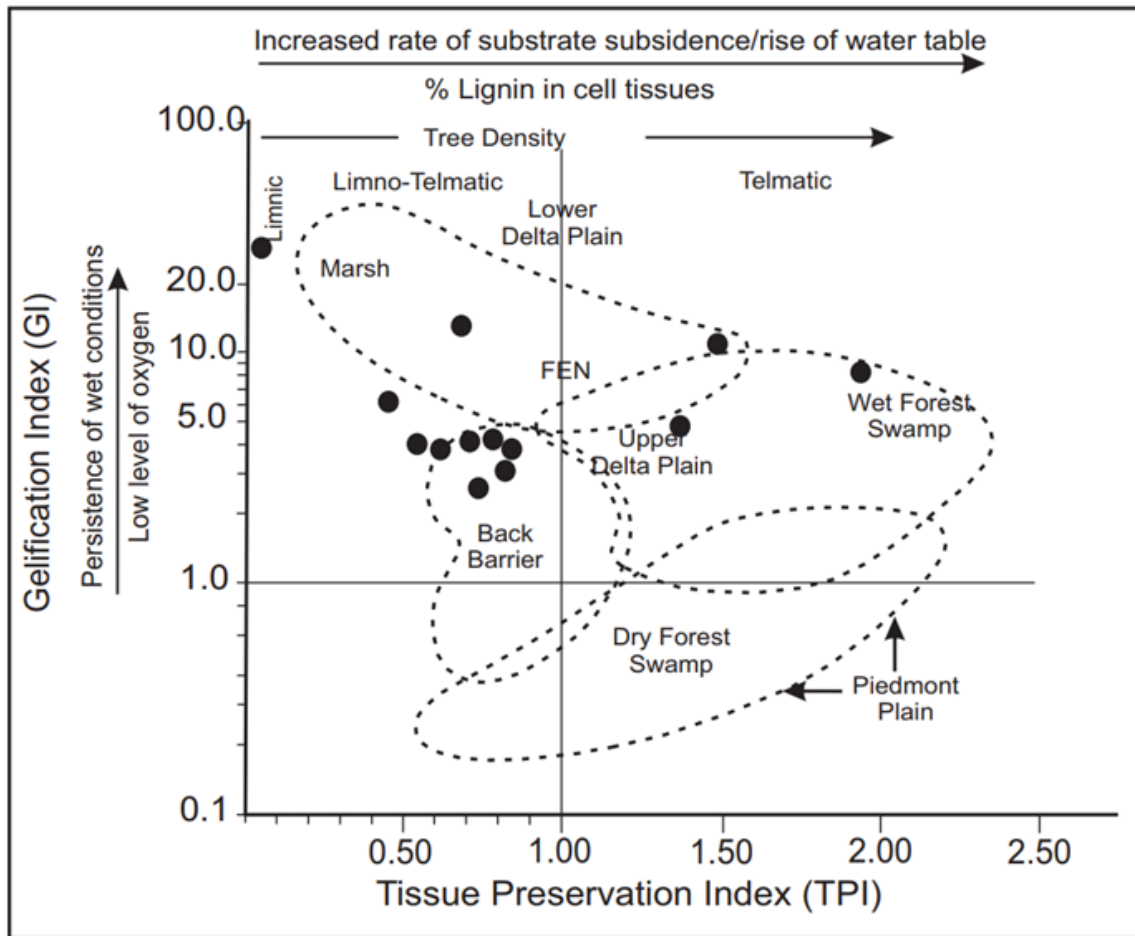


Fig. 13. Relationship of depositional settings and mire-type depicted by gelification (GI) and tissue preservation (TPI) indices (after Diessel, 1992).

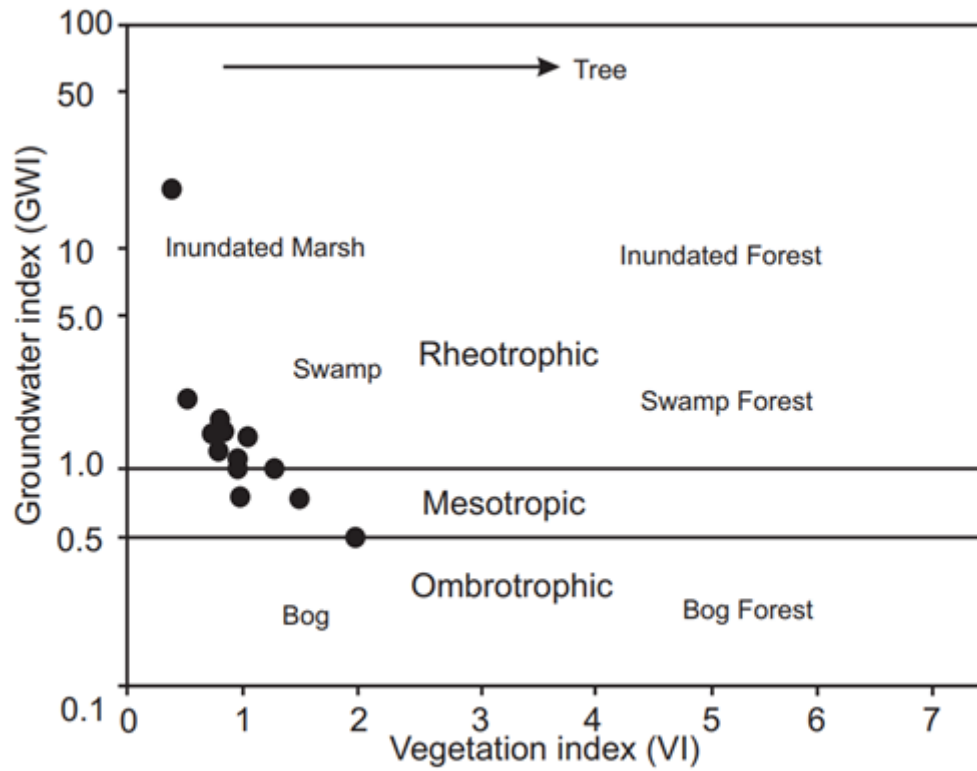


Fig. 14. Relationship between vegetation (VI) and ground water (GWI) indices showing the vegetation type and hydrological conditions (after Calder et al., 1991).

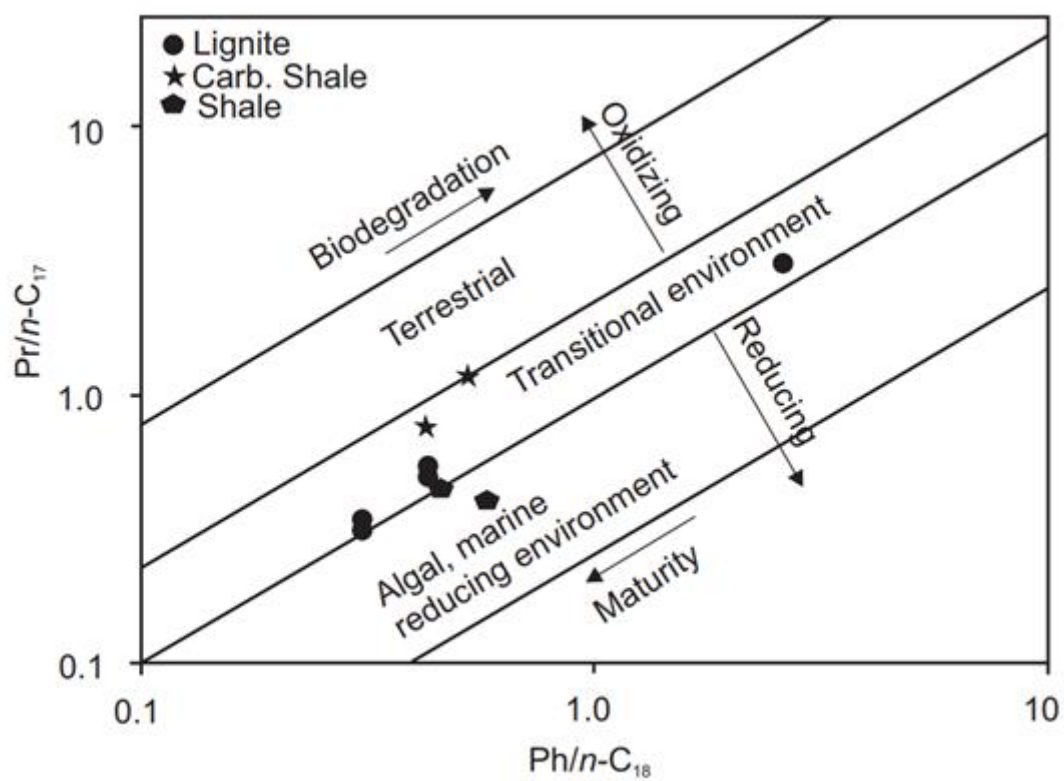


Fig. 15. Pristane/ n -C₁₇ vs. Phytane/ n -C₁₈ plot of the samples from Valia lignite mine.

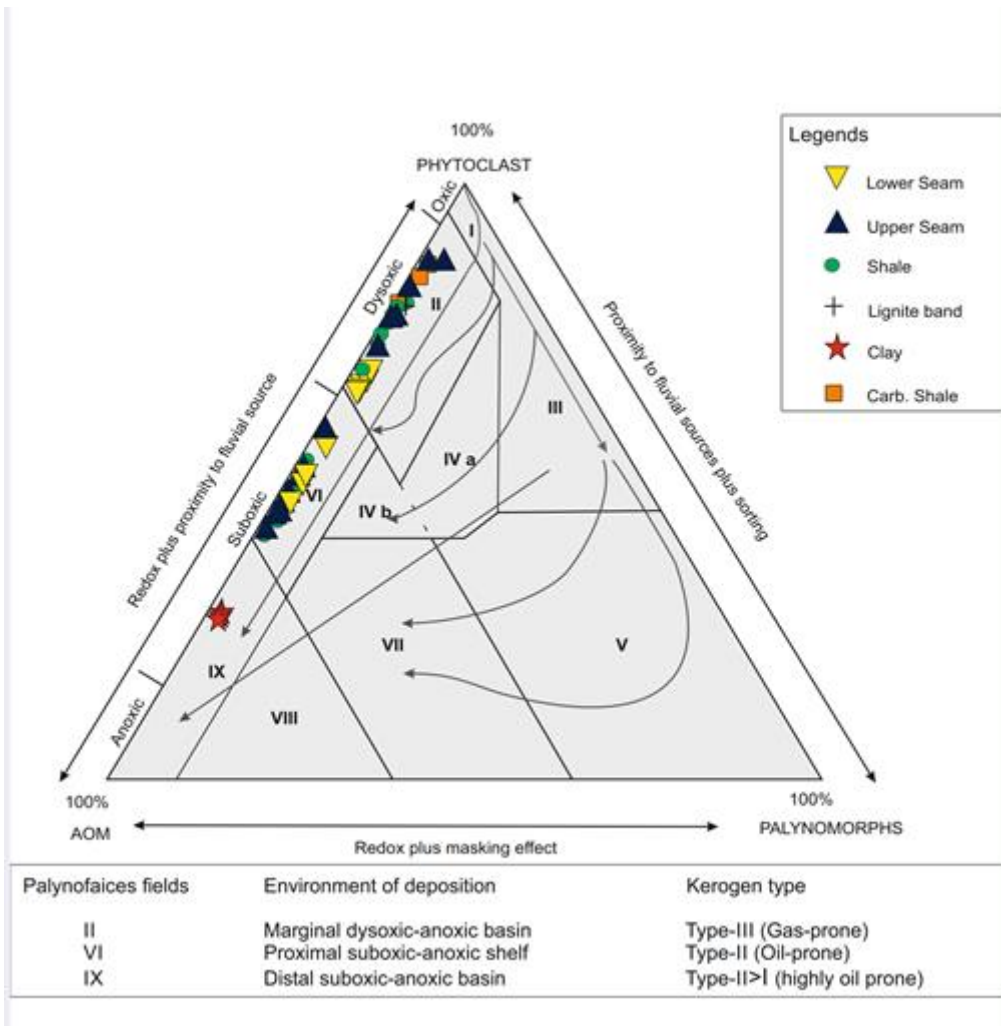


Fig. 16. A plot on Tyson's APP (Amorphous organic matter-palynomorph-phytoclast) diagram indicating the depositional fields and kerogen types for the studied samples.

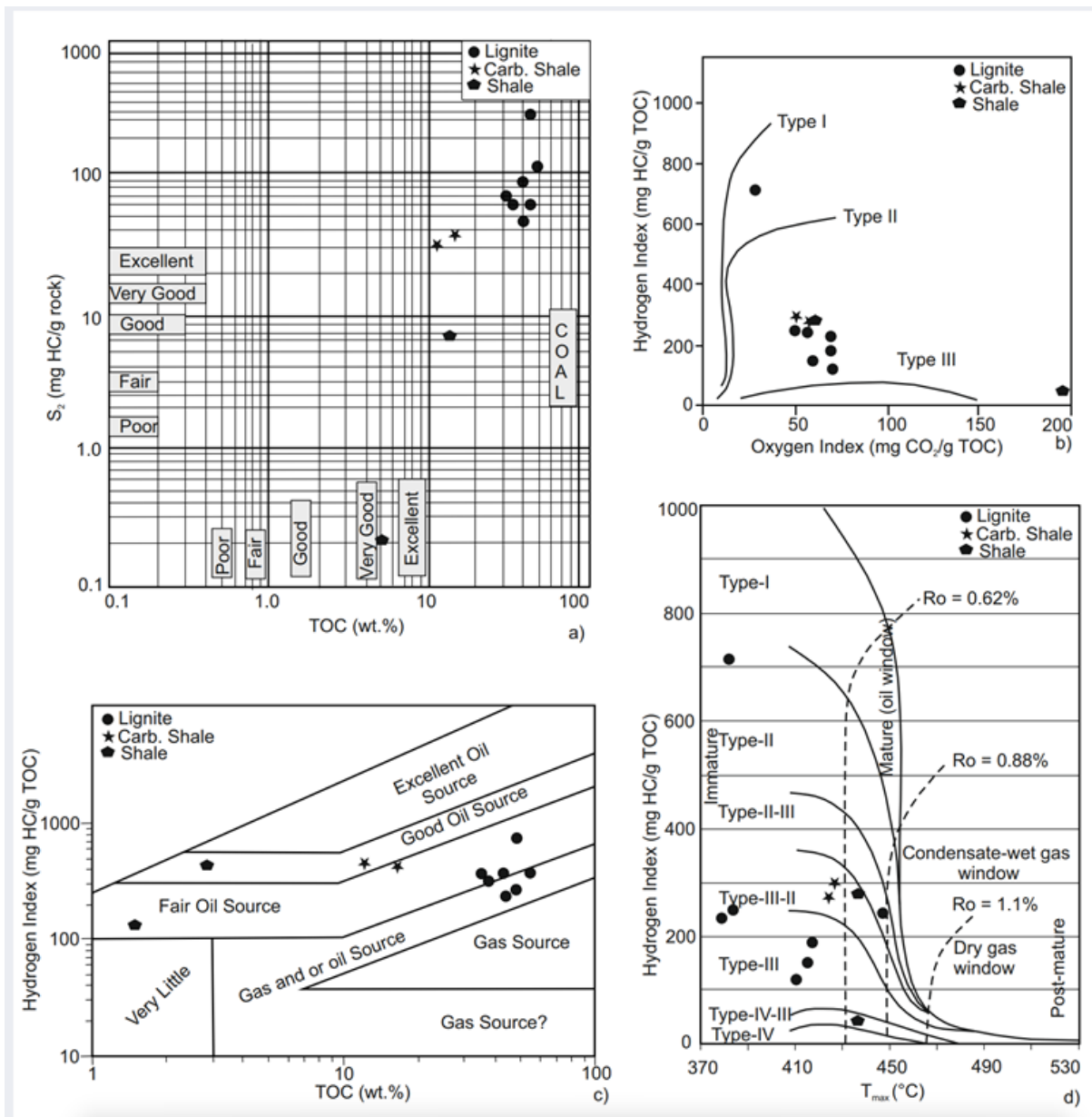


Fig. 17. Rock-Eval pyrolysis data plots of the Valia samples: a) S₂ vs. TOC, b) HI vs. OI, c) HI vs. TOC, d) HI vs. T_{max}.

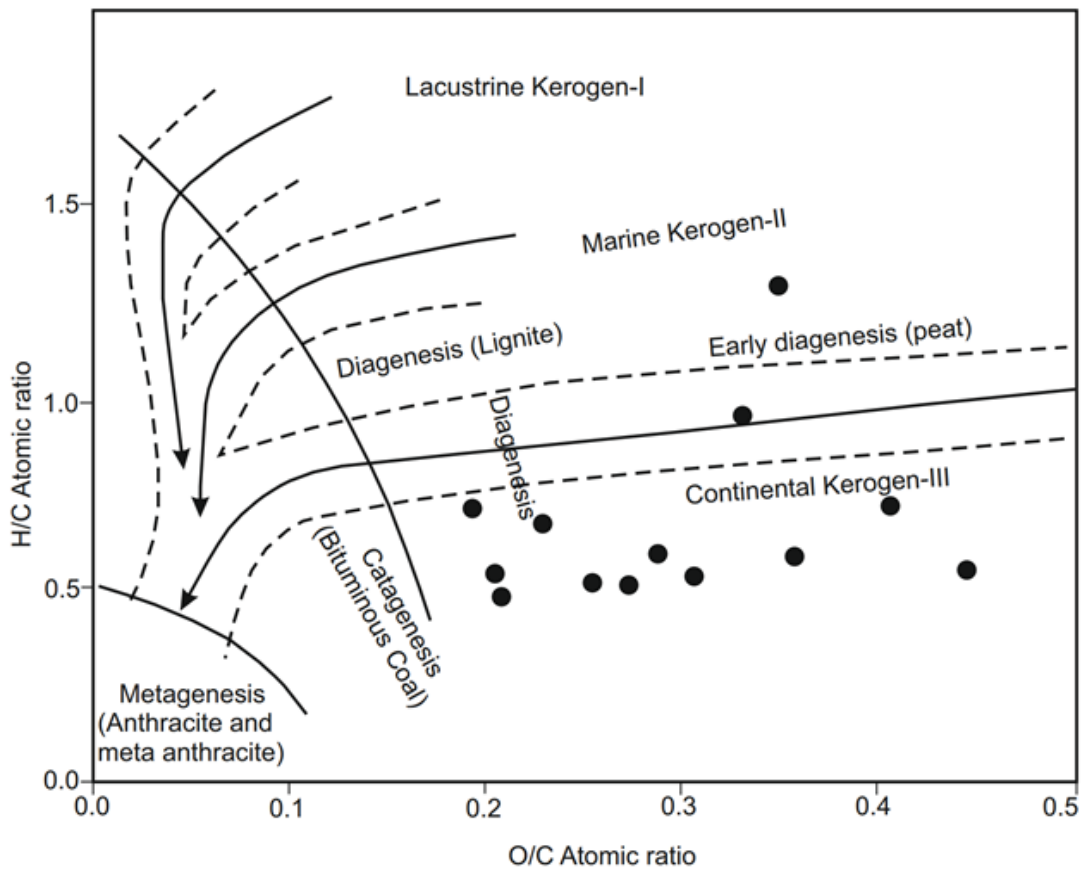


Fig. 18. Plot of atomic H/C vs. O/C ratios on Van Krevelen diagram for the studied Valia samples.